Spindle Assembly and Chromosome Segregation Requires Central Spindle Proteins in *Drosophila* Oocytes

Arunika Das,* Shital J. Shah,* Bensen Fan,* Daniel Paik,* Daniel J. DiSanto,* Anna Maria Hinman,* Jeffry M. Cesario,* Rachel A. Battaglia,* Nicole Demos,* and Kim S. McKim*,†,1

*Waksman Institute, Rutgers, The State University of New Jersey, New Jersey 08854, and †Department of Genetics, Rutgers, The State University of New Jersey, New Jersey 08854

ABSTRACT Oocytes segregate chromosomes in the absence of centrosomes. In this situation, the chromosomes direct spindle assembly. It is still unclear in this system which factors are required for homologous chromosome bi-orientation and spindle assembly. The *Drosophila* kinesin-6 protein Subito, although nonessential for mitotic spindle assembly, is required to organize a bipolar meiotic spindle and chromosome bi-orientation in oocytes. Along with the chromosomal passenger complex (CPC), Subito is an important part of the metaphase I central spindle. In this study we have conducted genetic screens to identify genes that interact with *subito* or the CPC component *Incenp*. In addition, the meiotic mutant phenotype for some of the genes identified in these screens were characterized. We show, in part through the use of a heat-shock-inducible system, that the Centralspindlin component RacGAP50C and downstream regulators of cytokinesis Rho1, Sticky, and RhoGEF2 are required for homologous chromosome bi-orientation in metaphase I oocytes. This suggests a novel function for proteins normally involved in mitotic cell division in the regulation of microtubule–chromosome interactions. We also show that the kinetochore protein, Polo kinase, is required for maintaining chromosome alignment and spindle organization in metaphase I oocytes. In combination our results support a model where the meiotic central spindle and associated proteins are essential for acentrosomal chromosome segregation.

KEYWORDS meiosis; synthetic lethal mutation; homolog bi-orientation; spindle; chromosome segregation; *Drosophila*

CHROMOSOMES are segregated during cell division by the spindle, a bipolar array of microtubules. In somatic cells, spindle assembly is guided by the presence of centrosomes at the poles. In this conventional spindle assembly model, the kinetochores attach to microtubules from opposing centrosomes and tension is established. This satisfies the spindle assembly checkpoint, which then allows the cell to proceed to anaphase (Musacchio and Salmon 2007). Cell division is completed by recruiting proteins to a midzone of antiparallel microtubules that forms between the segregated chromosomes, signaling furrow formation (Fededa and Gerlich 2012; D'Avino *et al.* 2015). However, spindle morphogenesis in oocytes of many animals occurs in the absence of centrosomes. This may contribute to the high rates of segregation errors that are maternal in origin and are a leading cause of miscarriages, birth defects, and infertility (Herbert *et al.* 2015). How a robust spindle assembles without guidance from the centrosomes is not well understood. While it is clear that the chromosomes can recruit microtubules and drive spindle assembly (Tseng *et al.* 2010; Dumont and Desai 2012), how a bipolar spindle is organized and chromosomes make the correct attachments to microtubules is not understood.

The *Drosophila* oocyte provides a genetically tractable system for the identification of genes involved in acentrosomal spindle assembly. Substantial evidence in *Drosophila* suggests that the chromosomes direct microtubule assembly, subsequent elongation of the spindle, and establishment of spindle bipolarity (Theurkauf and Hawley 1992; Matthies *et al.* 1996; Doubilet and McKim 2007). We have also shown that the kinesin-6 protein Subito, a homolog of human MKLP2

doi: 10.1534/genetics.115.181081
Manuscript received July 23, 2015; accepted for publication November 6, 2015; published Early Online November 11, 2015.
Supporting information is available online at www.genetics.org/lookup/suppl/doi:10.1534/genetics.115.181081/-/DC1.
[1]Corresponding author: Rutgers, the State University of New Jersey, Waksman Institute, 190 Frelinghuysen Rd., Piscataway, NJ 08854. E-mail: mckim@rci.rutgers.edu

with a role in cytokinesis (Neef *et al.* 2003), is also essential for organizing the meiotic spindle and the bi-orientation of homologous chromosomes (Giunta *et al.* 2002; Jang *et al.* 2005; Radford *et al.* 2012). Subito colocalizes with members of the chromosomal passenger complex (CPC), which is composed of the scaffolding subunit INCENP, the kinase Aurora B, and the targeting subunits Survivin (Deterin) and Borealin (Dasra) (Ruchaud *et al.* 2007). The CPC has a critical role in assembling the acentrosomal spindle and segregating chromosomes (Colombié *et al.* 2008; Radford *et al.* 2012). In addition, with Subito, the CPC localizes to the equatorial region of the meiotic metaphase I spindle and are mutually dependent for their localization (Jang *et al.* 2005; Radford *et al.* 2012). This equatorial region is composed of antiparallel microtubules and is a structure that includes a plethora of proteins (Jang *et al.* 2005). Assembling a central microtubule array may be a conserved mechanism to organize a bipolar spindle in the absence of centrosomes (Dumont and Desai 2012).

The meiotic central spindle, while assembling during metaphase, has several features and proteins associated with the midzone present during anaphase in mitosis. Indeed, Subito is required for the localization of the CPC to the midzone at anaphase (Cesario *et al.* 2006). The mitotic spindle midzone proteins function in anaphase and telophase to direct abscission, furrow formation, and cytokinesis (Glotzer 2005; D'Avino *et al.* 2015). The role of these proteins in the *Drosophila* acentrosomal meiotic spindle assembly pathway is unclear, however, since there is no cytokinetic function required at metaphase I and *Drosophila* does not extrude polar bodies (Callaini and Riparbelli 1996). It is possible that these proteins are loaded in the central spindle at metaphase for a function later in meiotic anaphase, as has been proposed for Centrosomin (Riparbelli and Callaini 2005). Alternatively, these central spindle proteins could be adapted for a new role, like Subito, in spindle assembly and/or bi-orientation of homologous chromosomes.

To identify and study the function of meiotic central spindle proteins, we carried out screens for genes that interact with *subito* (*sub*) and the CPC component *Incenp*. First, an enhancer screen was performed for mutations that are synthetically lethal with *sub*. Second, since synthetic lethality is a mitotic phenotype, a screen was performed for enhancement of the meiotic nondisjunction phenotype caused by a transgene overexpressing an epitope-tagged *Incenp* (Radford *et al.* 2012). In these screens we identified new mutations in CPC components (*Incenp*, *aurB*, *borr*), the Centralspindlin gene *tumbleweed* (*tum*), and the transcription factor *snail*. Mutations in at least 16 additional loci were also identified, and we directly tested candidate mitotic central spindle proteins for functions in meiosis. Several proteins were found to be required for microtubule organization and homologous chromosome bi-orientation during metaphase of meiosis I, including proteins in the Rho-GTP-signaling pathway required for cytokinesis such as TUM (RacGAP50C), Rho1, Sticky (Citron kinase homolog), and RhoGEF2. Not all mitotic midzone proteins are required for the meiotic central spindle, however, demonstrating meiosis-specific features of this structure. For example, Polo kinase may be required only for kinetochore function while the RhoGEF Pebble was not required for meiosis. In summary, this is the first documentation that proteins known to be required for anaphase/telophase and cytokinesis in mitotic cells are also essential in meiotic acentrosomal spindle assembly and chromosome bi-orientation.

Materials and Methods

Deficiency and mutagenesis screens for synthetic lethality

To test synthetic lethality of third chromosome mutations and deficiencies, *cn sub bw/CyO*; *e/ TM3*, *Sb* females were crossed to *Df/TM3*, *Sb* females (Supporting Information, Figure S1). The *cn sub bw/ +*; *Df/TM3* males were then crossed to *sub bw/CyO* or *cn sub/CyO* females to generate *cn sub bw/sub bw*; *Df/+* progeny. The frequency of these progeny was compared to *cn sub bw/sub bw*; *TM3/+* siblings to measure the synthetic lethal phenotype as a percentage of relative survival.

The mutagenesis screen was performed for the second chromosome using ethyl methanesulfonate (EMS). *y/y*$^{+}$*Y*; *sub*^{131} *bw sp/SM6* males were exposed to 2.5 mM EMS in 1% sucrose overnight. About 25 mutagenized males were mated to 50 *al dp b pr Sp bw/SM6* virgin females (Figure S2). Single *sub*^{131} *bw sp*/SM6* (asterisk denotes random mutations) males were mated with virgin *cn sub*^{1} *bw/SM6* females, and the progeny were scored for the absence of brown-eyed flies, which indicates a synthetic lethal interaction between the heterozygous EMS-induced mutation and the *sub* mutant. Initially, 51 synthetic lethal lines were isolated. Each line was retested twice by crossing *sub*^{131} *bw sp*/SM6a* sibling male progeny to *cn sub*^{1}*bw/SM6a* females and examining again for brown-eyed progeny. Eventually 19 lines carrying a synthetic lethal mutation (*sub*^{131} *bw sp*/SM6a*) were established and used for complementation testing and mapping.

Genetics, mapping, and complementation testing

To generate recombinant chromosomes for mapping or to remove the *sub*^{131} allele, we mated *sub*^{131} *bw sp*/SM6a* males to *al dp b pr cn c px sp/CyO* virgin females, collected *sub*^{131} *bw sp*/al d b pr cn c px sp* virgin females, and mated them to *al dp b pr Bl cn c px sp/CyO* males. Recombinants that were *al*$^{-}$ and *c*$^{+}$ were collected and, because these recombinants likely carried the *sub* mutant allele, were tested for synthetic lethality. In contrast, recombinants that retained the *c* mutation likely did not carry the *sub* mutant allele. These were used to evaluate whether the synthetic lethal mutation had a recessive lethal phenotype.

For establishing complementation groups, *sub*^{131} *bw sp*/SM6a* flies were crossed to *c px sp*/CyO* flies. A failure to complement was established by the absence of straight-winged (Cy+) progeny with a total of at least a hundred flies being scored. For some mutations we used deficiency mapping. Three deficiencies—*Df(2L)r10*, *Df(2L)osp29*, and *Df*

(2L)Sco[rv14]—failed to complement *22.64* and *27.18*. The allele of *snail* used for complementation was sna^{1}. One deficiency, *Df(2R)Exel7128*, failed to complement *15.173* and *16.135*. The alleles of *tum* used for complementation were tum^{AR2} and tum^{DH15}.

X-chromosome nondisjunction was measured by crossing females to *y Hw w* /$B^{S}Y$ males. The Y chromosome carries a dominant *Bar* allele such that XX and XY progeny are phenotypically distinguishable from exceptional XXY and XO progeny that received two or no X chromosomes from their female parent. Nullo-X and triplo-X progeny are inviable, which is compensated in nondisjunction calculations by doubling the number of XXY and XO progeny.

Generating germline clones by FLP-FRT

Males of the genotype *w/Y*; ovo^{D} *FRT40A/CyO* were mated to *y w hsFLP70*; *Sco/CyO* virgins, and *y w hsFLP70;*ovo^{D} *FRT40A/CyO* males were selected from the progeny. These were mated to either *22.64 pr FRT40A/CyO* (or *27.89*) virgins for the experiment or *b pr FRT40A/CyO* virgins for the control (Chou and Perrimon 1996). Third instar larval progeny from these crosses were heat-shocked at 37° for 1 hr on the fourth day. Female progeny of the genotypes *y w hsFLP*; ovo^{D} *FRT40A/ 22.64 FRT40A* and *y w hsFLP*; ovo^{D} *FRT40A/ b pr FRT40A* were yeasted for 3–4 days, and stage 14 oocytes were collected and analyzed.

Sequencing

DNA was extracted from a single fly (Gloor *et al.* 1993) and amplified using standard polymerase chain reaction. The gene of interest was amplified using specific primer sets spanning the length of the gene. This DNA was then sent for sequencing to Genewiz Inc. Since the stocks were balanced, the resulting sequence was analyzed using Align-X (Invitrogen) and Snapgene software for the presence of heterozygous SNPs indicating possible EMS-induced mutations.

Expression of RNAi in oocytes and quantification

Expression of short hairpin RNA lines designed and made by the Transgenic RNAi Project at Harvard (TRiP) was induced by crossing each RNAi line to either $P\{w^{+mC} = tubP\text{-}GAL4\}LL7$ for ubiquitous expression or $P\{w^{+mC} = matalpha4\text{-}GAL\text{-}VP16\}V37$ for germline-specific and oocyte expression (referred to as "drivers"). The latter is expressed throughout oogenesis starting late in the germarium (Radford *et al.* 2012). For expression of *tum* RNAi we used *P{GAL4-Hsp70.PB}89-2-1*. In this method, 2-day-old adult females were yeasted for 2 days with males and then heat-shocked for 2 hr at 37°. They were allowed to recover for 3 1/2 hr, and then oocytes were collected and fixed. At this time point the oocytes that were at approximately stages 10–11 at the time of heat shock were being laid as mature oocytes. Later time points did not yield sufficient quantities of oocytes in the *tum* RNAi as oogenesis had arrested by then. *tum* RNAi females were sterile for 72 hr after heat shock whereas wild type regained fertility soon after heat shock.

For reverse transcriptase quantitative PCR, total RNA was extracted from late-stage oocytes using TRIzol Reagent (Life Technologies). Complementary DNA (cDNA) was consequently prepared using the High Capacity cDNA Reverse Transcription Kit (Applied Biosystems). The qPCR was performed in either a StepOnePlus (Life Technologies) or Eco (Illumina) real-time PCR system using the following TaqMan Gene Expression Assays (Life Technologies): Dm01823196_g1 (*polo*), Dm01794608_m1 (*Rho1*), Dm018202757_g1 (*sticky*), Dm01794707_m1, (*RhoGEF2*), and Dm01822327_g1 (*pebble*).

Antibodies and immunofluorescent microscopy

Stage 14 oocytes were collected from 50 to 200, 3- to 4-day-old yeast-fed nonvirgin females by physical disruption in a common household blender in modified Robb's media (Theurkauf and Hawley 1992; McKim *et al.* 2009). The oocytes were fixed in either 100 mM cacodylate/8% formaldehyde fixative for 8 min or 5% formaldehyde/heptane fixative for 2.5 min and then their chorion and vitelline membranes were removed by rolling the oocytes between the frosted part of a slide and a coverslip (McKim *et al.* 2009). For FISH, oocytes were prepared as described (Radford *et al.* 2012). Oocytes and embryos were stained for DNA with Hoechst 33342 (10 μg/ml) and for microtubules with mouse anti-α-tubulin monoclonal antibody DM1A (1:50), directly conjugated to FITC (Sigma, St. Louis) or rat anti-α-tubulin monoclonal antibody (1:75) (Millipore). Additional primary antibodies were rat anti-Subito antibody (used at 1:75) (Jang *et al.* 2005), rat anti-INCENP (1:400) (Radford *et al.* 2012), rabbit anti-TUM (1:50) (Zavortink *et al.* 2005), rabbit anti-SPC105R (1:4000) (Schittenhelm *et al.* 2007), rabbit anti-Sticky (1:50) (D'Avino *et al.* 2004), and mouse monoclonal anti-Rho1 (P1D9, 1:50) (Magie *et al.* 2002). These primary antibodies were combined with either a Cy3 or Cy5 secondary antibody pre-absorbed against a range of mammalian serum proteins (Jackson Immunoresearch, West Grove, PA). FISH probes used were the AACAC repeat (second chromosome) and dodeca repeat (third chromosome). Oocytes were mounted in SlowFade gold (Invitrogen). Images were collected on a Leica TCS SP5 or SP8 confocal microscope with a 63×, numerical aperture 1.4 lens. Images are shown as maximum projections of complete image stacks followed by merging of individual channels and cropping in Adobe Photoshop (PS6).

Results

sub mutants interact with multiple third chromosome loci including Deterin (Survivin) and pavarotti (MKLP1)

Null mutants of *sub* are viable but female sterile (Giunta *et al.* 2002). CPC members INCENP and Aurora B are mislocalized in the larval neuroblasts of *sub* mutants, which may be the reason why a reduction of INCENP or Aurora B dosage by 50% causes *sub* homozygotes to die (Cesario *et al.* 2006). This observation suggests that the *sub* mutant is a sensitized genetic background in which to perform forward genetic

screens to identify mitotic proteins with possible functions in meiosis similar to the CPC or Subito. Thus, we performed screens for mutations that show a dominant lethal interaction with *sub*, also known as "synthetic lethality" (Figure S1 and Figure S2). The advantage of these screens is that we can recover mutations in essential genes and identify genes encoding central spindle proteins even if there is no direct physical interaction.

On the third chromosome we screened 81 deficiencies obtained from Bloomington Stock Center for synthetic lethality, covering ~75% of the chromosome. Synthetic lethality was calculated as a ratio of sub^1/sub^{131};*Df*/+ to sub^1/sub^{131};+/+ progeny. Seven deficiencies—*Df(3L)ZN47*, *Df(3R)23D1*, *Df(3R)DG2*, *Df(3L)rdgC-co2*, *Df(3L)GN24*, *Df(3R)Exel9014*, and *Df(3L)ri-XT1*—that displayed synthetic lethal interaction with *sub* at viability rates between 0–10% were identified (Table 1). Three additional deficiencies—*Df(3R)Antp17*, *Df(3L)emc-E12*, and *Df(3R)BSC43*—exhibited a milder synthetic lethal interaction with a viability rate between 10 and 30% (Table 1).

For each of the seven deficiencies with the strongest synthetic lethal phenotype, we looked at sets of overlapping deficiencies and specific mutations to identify candidate genes. *Df(3R)DG2* uncovers the gene *Deterin* (also known as *survivin*), which we expect to be synthetic lethal with *sub* similar to the other members of the CPC. A null allele of *Deterin* was tested and also exhibited a synthetic lethal interaction (4% sub^1/sub^{131};Det^{e01527}/+ progeny; n = 184). Deficiency *Df(3L)rdgC-co2* uncovers *polo*, which we expected to be synthetic lethal based on previous results (Cesario *et al.* 2006). Within *Df(3L)GN24* we tested six smaller deficiencies and found synthetic lethality with *Df(3L)Exel9000*. Within this deficiency is *pavarotti*, which encodes the *Drosophila* homolog of MKLP1 that localizes to the central spindle in both mitosis and meiosis similar to Subito (Adams *et al.* 1998; Minestrini *et al.* 2003; Jang *et al.* 2005). A null allele of *pavarotti* also was synthetic lethal with *sub* (0% sub^1/sub^{131}; pav^{B200}/+ progeny; n = 69).

Two of the deficiencies identified as synthetic lethal with *sub*, *Df(3R)Exel9014*, and *Df(3L)ri-XT1* disrupt the kinetochore protein-encoding gene *Spc105R* (Table 1). *Df(3R)Exel9014* does not delete *Spc105R*, but the chromosome carries a second mutation that is a null allele, $Spc105R^1$ (Schittenhelm *et al.* 2009). One of two smaller deficiencies within *Df(3L)ri-XT1*, *Df(3L)BSC452*, also deletes *Spc105R* and has a synthetic lethal phenotype. We directly tested synthetic lethality with a $Spc105R^1$ chromosome that lacked *Df(3R)Exel9014*. $Spc105R^1$ on its own was not synthetic lethal with *sub* (n = 253). We also tested two additional kinetochore mutants, but neither *mis12* (n = 337) nor *spc25* (n = 131) were synthetic lethal with *sub*. These results suggest that there is no synthetic lethal interaction between *sub* and kinetochore mutants. *Df(3R)Exel9014* and *Df(3L)ri-XT1* must interact with *sub* because of loci other than *Spc105R*.

For two of the deficiencies, *Df(3L)ZN47* and *Df(3R)23D1*, we did not identify a smaller interacting region. It is possible that the interaction lies in a gene disrupted only by the larger deficiency. Alternatively, the genetic interaction may involve haploinsufficiency for more than one gene within the larger deficiency. There are also possibly more complex interactions of positive and negative regulators. In this case, a smaller deficiency could have a less severe synthetic lethal phenotype than a point mutant. This was observed with deletions of *pav*. While a *pav* mutation and *Df(3L)GN24* had severe synthetic lethal phenotypes, the smaller deficiency *Df(3L)Exel9000* had a relatively mild synthetic lethal phenotype.

Overall, in addition to confirming genetic interactions between *sub* and *polo*, *pav* or *Det*, the third chromosome deficiency screen for synthetic lethality identified at least seven additional interacting loci.

Mutagenesis screen for synthetic lethal mutants on the second chromosome reveals new alleles of CPC genes and centralspindlin component Tumbleweed

A mutagenesis screen of the second chromosome was done to identify genes that genetically interact with *sub*. We screened 5314 second chromosomes mutagenized with EMS and isolated 19 lines with a synthetic lethal phenotype (*Materials and Methods*) (Figure S2). We expected to obtain alleles of the CPC since three of its members—*Incenp*, *aurB*, and *borr*—are on the second chromosome. Complementation testing with deficiencies uncovering these genes and existing mutants revealed three alleles of *Incenp*, two of *aurB*, and one of *borr* (Table 2). Most of these mutations were also homozygous lethal. However, $Incenp^{18.197}$ is a hypomorphic allele that causes recessive sterility and not lethality. The rest of the mutations were put into 11 complementation groups. There are 2 groups with two alleles each (*22.64*, *27.18* and *15.173*, *16.135*) and 9 that are represented by one allele each (Table 2).

Some synthetic lethal mutations that complemented all CPC mutants were genetically mapped (Table 2). We picked two types of recombinants—those that also retained the *sub* mutation so that the synthetic lethal mutation could be mapped and those that did not have the *sub* mutation—to determine if the mutation had a recessive phenotype, such as lethality or sterility. A detailed example of this approach is described in File S1 for the synthetic lethal mutation *27.89*.

Mutation *27.89* was mapped between *dp* and *b* on chromosome 2R. Using SNP mapping, the synthetic lethal mutation was mapped to a 300-kb region (File S1, Figure S3, and Figure S4). Surprisingly, it is possible that *27.89* is homozygous lethal but viable when heterozygous to a deficiency (Figure S5), although we have not excluded a second lethal mutation on the *27.89* chromosome. To examine if *27.89* has a germline phenotype, we generated germline clones to collect *27.89* homozygous oocytes to determine if there was an effect on meiosis. In fact, homozygous *27.89* germline clones failed to develop into mature oocytes. This inability to generate mature germline clones is a phenotype shared by other

Table 1 Deficiencies that are synthetic lethal with *sub* and/or dominantly enhance *Incenp^{myc}*

Deficiency	Cytology	Viability[a]	Total[a]	% X-nondisjunction[b]	Total[b]	Candidate genes
sub				20.3	1438	
+				1.3	158	
Df(3L)emc-E12	61A;61D3	30.1	272	22.6	257	*fwd*
Df(3L)ED4177	61C1;61E2	67.0	309	2.6	1440	*fwd*
Df(3L)GN24	63F6-63F7;64C8-64C9	0	118	1.2	1027	*pavarotti*
Df(3L)Exel9000	64A10;64A12	30.1	359	5.3	219	*pavarotti*
Df(3L)ZN47	64C4-64C6;65D2	0	98	2.1	391	*Mad2*, *RCC1*
Df(3L)rdgC-co2	77A1;77D1	7.3	191			*polo*
Df(3L)ri-XT1	77E2-77E4;78A2-78A4	6.1	70	12.2	460	*Spc105R*, *pitsire*
Df(3L)BSC452	77E1;77F1	39	163	13.1	565	
Df(3L)BSC449	77F2;78C2	122	180	4.8	565	
Df(3R)Antp17	84A1-84A5;84D9	16.7	28			
Df(3R)DG2	89E1-89F4;91B1-91B2	0	36	0.0	297	*Deterin*
Df(3R)ED5780	89E11;90C1			8.7	577	
Df(3R)BSC43	92F7;93B6	10.1	89	0.0	439	
Df(3R)23D1	94A3-94A4;94D1-94D4	0	175	6.1	457	
Df(3R)Exel6191	94A6;94B2	113.3	224	3.8	311	
Df(3R)Exel6273	94B2;94B11	112.3	155	4.5	532	
Df(3R)ED6091	94B5;94C4	158.1	191	0.0	156	
Df(3R)Exel6192	94B11;94D3	111.1	133	6.0	807	ND
Df(3R)Exel9013	95B1;95B5	132.8	288	8.4	1197	ND
Df(3R)Exel9014	95B1;95D1	0	49	11.1	2234	ND
Df(3R)Exel6196	95C12;95D8	140.6	77	6.5	2043	ND

[a] Percentage viability was calculated from the ratio of *sub^{131}/sub^{1};Df/+::sub^{131}/sub^{1};+/+* flies obtained (Figure S2).
[b] X-chromosome nondisjunction was measured by crossing females to *y Hw w/B^{S}Y* males (*Materials and Methods*).

mutations isolated in the screen such as *Incenp*, *aurB*, and *tumbleweed*, which are involved in the early mitotic cell divisions that occur pre-oogenesis. This indicates that *27.89* may play a role in cell division.

Mutation *22.64* was mapped to the interval between *b* and *pr* and, based on complementation to deficiencies, we found that *22.64* and *27.18* failed to complement existing alleles of *snail*, which encodes a zinc finger containing a transcriptional repressor (Ashraf *et al.* 1999; Ashraf and Ip 2001). This was a surprising finding because *snail* has not previously been shown to regulate spindle assembly. An analysis of mature oocytes using germline clones has revealed that *snail* mutants do not grossly affect meiotic spindle assembly (Figure S6). Further work is necessary to address why *snail* mutations enhance the *sub* mutant phenotype and if *snail* has a role in meiotic or mitotic spindle function. Interestingly, a *Drosophila* paralog of Snail, Worniu, has been shown to regulate cell cycle progression in neuroblasts (Lai *et al.* 2012).

Both *15.173* and *16.135* genetically mapped to a region on chromosome 2R between *cn* and *c* and failed to complement a deficiency in this region, *Df(2R)Exel7128*. Based on this mapping, we found that both mutations failed to complement existing alleles of *tum*, which encodes the *Drosophila* homolog of RacGAP50C (Goldstein *et al.* 2005). RacGAP50C is a Centralspindlin component that, as described earlier, also includes Pavarotti. Thus, all known members of two complexes, the CPC and Centralspindlin, genetically interact with *sub*. This is consistent with previous observations that Subito, Incenp, and RacGAP50C colocalize at the central spindle during mitosis (Cesario *et al.* 2006) and meiosis (Jang *et al.* 2005). Below are the results from analyzing the meiotic phenotype of oocytes depleted for RacGAP50C.

Mutations that enhance the dominant meiotic chromosome segregation phenotype of an Incenp allele

While the synthetic lethal screens revealed genes that interact with *sub*, these genes may not function in meiosis. To test interacting genes for a function in meiosis, we determined if they enhanced the nondisjunction phenotype of a transgene expressing the CPC member *Incenp* tagged with the *myc* epitope at its N terminus (*UASP:Incenp^{myc}*). Females expressing *UASP:Incenp^{myc}* with *nos-GAL4:VP16* in addition to the endogenous alleles show ~1% X-chromosome nondisjunction. Females also heterozygous for a null allele of *sub* show ~20% X-chromosome nondisjunction (Radford *et al.* 2012) (Table 1). It is not known if the phenotype arises from the N-terminal tag or overexpression of Incenp. We used *UASP:Incenp^{myc}* to screen for mutations that dominantly enhance the nondisjunction phenotype, similar to *sub*.

We tested deficiencies that showed a synthetic lethal interaction with *sub* (Table 1). Using a cutoff for enhancement of 4% increase over the control, 10 deficiencies showed an increase in nondisjunction ranging from 5 to 19% over control levels (Table 3). This assay appears to be more sensitive than the synthetic lethal phenotype for detecting interactions. For example, the strong nondisjunction phenotype of *Df(3L)emc-E12* contrasts with the mild synthetic lethal phenotype. Similarly, while *Df(3R)BSC452* had a milder synthetic lethal phenotype than the larger *Df(3R)ri-XT1*, it had a similar nondisjunction phenotype with *UASP:Incenp^{myc}*.

Table 2 Mutations obtained from EMS screen of the second chromosome

Complementation groups	Mutant localization	Allele	Phenotype[a]	Mutation
Incenp	43A2-43A3	22.68	Lethal	Q611-Stop
		47.125	Lethal	ND
		18.197	♀ Sterile	P746L
aurB	32B2	35.33	Lethal	L166F
		49.149	Lethal	Q95-Stop
borr		44.356	Lethal	Lost
snail	35D2	22.64	Lethal	ND
		27.18	Lethal	Q275-Stop
tumbleweed	50C6	15.173	Lethal	P463L
		16.135	Lethal	ND
6	31B1-32D1	27.89	Lethal	
7	34D1-43E16	27.88	viable	
8	ND	48.116	Lethal	
9	25A2 – 34D1	44.13	Lethal	
10	ND	46.10	Lethal	
11	ND	47.90	ND	
12	ND	47.134	ND	Lost
13	ND	49.178	ND	Lost
14	ND	10.33	ND	

[a] Based on phenotype of recombinant chromosome lacking the *subito* mutation.

Taking into account that some of these deficiencies overlap, these experiments identified at least six loci that genetically interact with *UASP:Incenp^{myc}*. These results suggest that some of the deficiencies identified as synthetic lethal also have at least one gene required for meiotic chromosome segregation.

In addition, we tested several candidate genes for enhancement of *UASP:Incenp^{myc}* (Table S1). A mutation in *non-claret disjunctional* (*ncd*), which encodes a kinesin-14 motor protein, was notable because it enhanced as strongly as *sub*. The groups of genes that most consistently enhanced *UASP:Incenp^{myc}* were Cyclin B and its regulators. Also relevant to the current study is the finding that mutants in cytokinesis genes such as *four wheel drive* (*fwd*), which encodes phosphatidylinositol (PI) 4-kinase III β (Polevoy *et al.* 2009), and *twinstar*, which encodes cofilin (Gunsalus *et al.* 1995), enhanced *UASP:Incenp^{myc}*. Some mutants had surprisingly weak enhancement phenotypes, such as *pav*, *Df(3L)Exel9000* that deletes *pav* and *tum*, which are strongly synthetic lethal. Other notable mutations that did not interact with *UASP:Incenp^{myc}* were in the central spindle component gene *feo* (encodes PRC1) and the checkpoint genes *BubR1* and *zw10*. These results suggest that the enhancement of *UASP:Incenp^{myc}* depends on a specific defect. Indeed, there was evidence for allele-specific interactions, with mutations in genes such as *fzy*, which encodes a Cdc20 homolog; *ord*, which encodes a nonconserved cohesion protein, *spc25*, which encodes a kinetochore protein; and *Incenp*. Furthermore, a *fwd* mutant enhanced *UASP:Incenp^{myc}* while a deficiency, *Df(3L)ED4177*, had a weaker phenotype. These results suggest that specific types of alleles may cause enhancement of *UASP:Incenp^{myc}*. It is possible that all the genes that interact with *UASP:Incenp^{myc}* affect the localization or regulation of *sub* (see *Discussion*).

Polo kinase is required for karyosome maintenance and homologous chromosome bi-orientation at metaphase I

In the previous sections, we identified genes that genetically interact with *sub* and *Incenp*. To determine if any are required during meiosis I for chromosome segregation, we examined oocytes lacking some of these proteins for meiotic defects. Loss of these genes might be expected to have a phenotype similar to *sub* mutants, with defects in spindle bipolarity and homolog bi-orientation.

Mutants of *polo* are synthetic lethal with *sub* (Cesario *et al.* 2006). Since *polo* mutants are recessive lethal, we used *polo* RNAi (TRiP GL00014 and GL00512) to test the function of Polo in acentrosomal spindle assembly and chromosome segregation. Expression of both short hairpin RNA (shRNA) lines using ubiquitous *P{tubP-GAL4}LL7* resulted in lethality, suggesting that the protein had been knocked down by the shRNA. Oocyte-specific shRNA expression was achieved using *matalpha4-GAL4-VP16*, and this resulted in sterility and knockdown of the messenger RNA as measured by qRT-PCR (Table S2 and Figure S7).

In wild-type oocytes, the chromosomes cluster together in a spherical mass referred to as the karyosome in the center of a spindle with well-defined poles and a central spindle containing Subito and the CPC (Figure 1, A and G). In *polo* GL00014 RNAi oocytes, there were defects in both chromosome and spindle organization. There were multiple karyosome masses (2–5) in most oocytes (Figure 1B) (69%; $n = 31$). In addition, there were defects in spindle microtubules that we have classified into three types. First, 55% of the oocytes had disorganized spindles with characteristics like frayed microtubules, untapered spindle poles, and displaced karyosomes (Figure 1B). Second, 39% of the spindles appeared "hollow," composed primarily of central spindle microtubules and few or no

Table 3 Frequency of mono-orientation in oocyte knockouts of central spindle proteins

Genotype	AACAC % mono-orientation (*n*)[a]	DODECA % mono-orientation (*n*)[b]	*P*-value[c] (AACAC)	*P*-value[c] (DODECA)	Total
Wild type	4 (2)	0	NA	NA	45
Wild type (HS)[d]	5.5 (1)	5.5 (1)	NA	NA	18
tum HMS01417 (HS)[d]	50 (10)	45 (9)	0.004	0.009	20
Rho1 HMS00375	35 (9)	15 (4)	0.001	0.019	26
sticky GL00312	27 (6)	18 (4)	0.013	0.015	22
RhoGEF2 HMS01118	20 (5)	13 (3)	0.045	0.039	24
pbl GL01092	0	0	NS	NS	15
polo GL00014	61.9 (13)	47.6 (10)	0.009	0.01	21

[a] Percentage of total oocytes with second chromosome AACAC probe mono-oriented.
[b] Percentage of total oocytes with third chromosome Dodeca probe mono-oriented.
[c] Fisher's exact test was used to calculate the *P*-values compared to wild type.
[d] HS = heat shock: These values were obtained from independent experiments with the heat-shock driver.

kinetochore microtubules, those microtubules ending at the chromosomes (Figure 1C). Third, 16% of the oocytes had mono- or tripolar spindles (Figure 1D). Localization of the central spindle proteins INCENP and Subito was not affected (Figure 1H), suggesting that Polo is not required for central spindle assembly. Similar observations were made when the other shRNA, GL00512, was expressed (Figure 1I). The multiple karyosome phenotype (78%; $n = 14$) and spindle defects (Table S2) were observed at similar frequencies with the two shRNAs.

Polo accumulates at the kinetochores during meiotic metaphase of *Drosophila* oocytes (Jang *et al.* 2005). Therefore, we examined the centromeres and kinetochores directly in Polo knockout oocytes. At metaphase in wild-type oocytes, the centromeres are attached to microtubules and oriented toward the two poles while the central spindle forms between them with proteins like Subito and INCENP localized in a ring around the karyosome. The kinetochore protein SPC105R localized normally in GL00014 oocytes (Figure 2A), suggesting that Polo is not required for kinetochore assembly. With an average of 6.5 SPC105R foci per oocyte compared to 6.7 in wild type, these results also show that Polo is not required for cohesion at the centromeres at metaphase I (Figure 2B), in contrast to a recent report in mouse (Kim *et al.* 2015).

In wild-type oocytes, each pair of homologous centromeres orients toward opposite poles (known as bi-orientation). To test if *polo* knockdown oocytes have bi-orientation defects, we performed FISH on *polo* RNAi oocytes with probes to the second (AACAC) and third (Dodeca) chromosome heterochromatin. Wild-type oocytes normally shows the second and third chromosome signals oriented toward opposite poles (Figure 2C and Table 3). In *polo* knockdown oocytes, the second and third chromosomes were frequently mono-oriented compared to wild type (Figure 2, D–F; Table 3). Due to the separated karyosome phenotype, in some cases these defects were observed in oocytes where the second and third chromosomes were in different masses with their own spindles. Importantly, in most cases where the karyosomes had separated, the homologous chromosome pairs were in the same mass, indicating that the cohesion holding the bivalents together had not been released. These results show that Polo is required for microtubule attachment, chromosome bi-orientation, and karyosome structure, but is not required for central spindle function.

Centralspindlin is required for meiotic spindle organization and homologous chromosome bi-orientation

We identified the Centralspindlin components *pav* and *tum* as synthetic lethal mutations with *sub*. The role of the Centralspindlin proteins in mitotic spindle midzone formation and stabilization leading to cytokinesis is well documented (Guse *et al.* 2005; D'Avino *et al.* 2006; Pavicic-Kaltenbrunner *et al.* 2007; Simon *et al.* 2008). Their contribution to acentrosomal spindle assembly, however, has not been characterized. To test the role of the Centralspindlin complex in oocyte meiotic spindle assembly, we expressed shRNA against both *tum* and *pav* (HMS01417 and HMJ02232, respectively) (Ni *et al.* 2011) with *GAL4*::*VP16-nos.UTR*, which expresses GAL4 with the germline-specific promoter from the *nanos* gene (Rorth 1998). Both lines failed to generate mature oocytes, probably due to cytokinesis defects in the mitotic germline divisions, which would also preclude using the FLP-FRT system to generate germline clones. To circumvent this problem, we expressed each shRNA with *matalpha4-GAL-VP16*, which expresses throughout most of the meiotic prophase but, importantly, after premeiotic S phase (Radford *et al.* 2012). However, these two shRNAs expressed with *matalpha4-GAL-VP16* also produced very few mature oocytes, indicating a role for these proteins in oogenesis that prevented analysis of their meiotic function.

Because of the requirement for *tum* and *pav* in oogenesis, we developed an alternative method to knock down gene expression in oocytes. We chose to focus on *tum* with the goal of knocking down expression after its requirement in oogenesis, but prior to spindle assembly in mature oocytes. To achieve this, a heat-shock-inducible driver (*P{GAL4-Hsp70.PB}89-2-1*) was used to express *tum* shRNA (Figure 3A). The *Drosophila* oocyte undergoes 14 developmental stages to form a mature oocyte (Spradling 1993). Therefore, application of heat shock to a female will result in induction of RNAi in all stages present at the time. At 5 hr after induction of

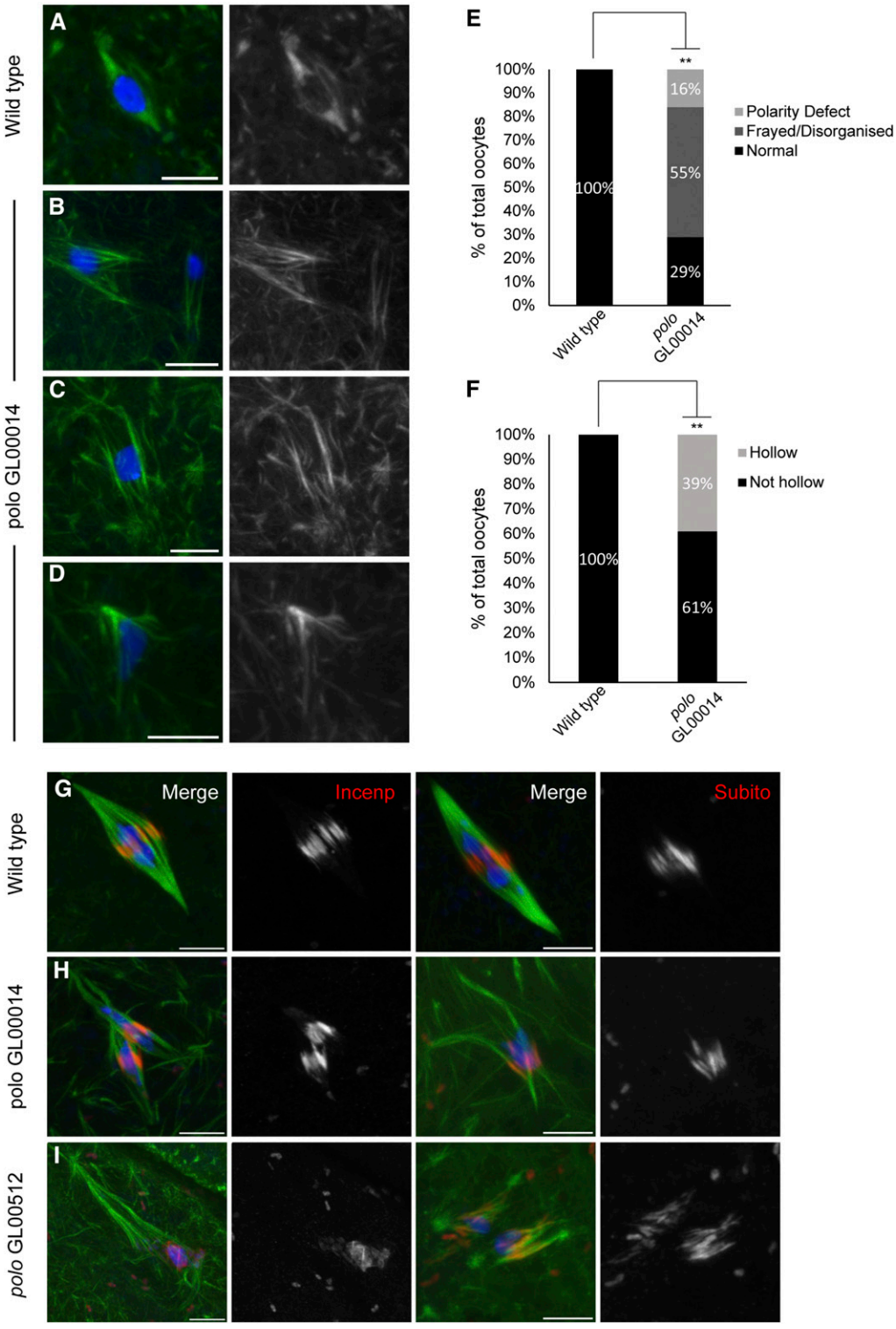

Figure 1 Polo is required for karyosome and spindle organization at meiotic metaphase I. DNA is in blue, INCENP or Subito is in red, and tubulin is in green. (A) A wild-type bipolar spindle and (B–D) *polo* RNAi oocytes showing monopolar, frayed/disorganized, and hollow spindles, respectively. (E and F) Spindle defects in *polo* RNAi (n = 33) oocytes compared to wild type (n = 13). Percentage of oocytes with disorganized (E) or hollow (F) spindles are graphed separately. Asterisks denote significantly higher spindle defects (for E, P = 0.001; for F, P = 0.009). (G) Wild-type bipolar spindle showing either INCENP or Subito staining at meiotic central spindle. (H and I) *polo* GL00014 or GL00512 RNAi oocytes showing INCENP and Subito localization. Bars, 5 μm.

tum shRNA by heat shock, the adult females produced inviable embryos, suggesting that they had stage 14 oocytes depleted of TUM. This was confirmed using an antibody to TUM, which showed an absence of TUM protein on the spindle in a majority of the heat shock treated oocytes (Figure S8). At times greater than 5 hr after heat shock, in which stage 14 oocytes would have been at stage 10 or earlier at the time of heat shock, stage 14 oocytes were not produced. These results suggest that oocytes depleted of TUM at stage 10 or earlier fail to develop. With the 5-hr time point, however, we could investigate *tum* knockdown oocytes for defects in acentrosomal meiotic spindle assembly and chromosome segregation.

Similar to wild type, in heat-shocked wild-type oocytes or *tum* shRNA oocytes that were not heat-shocked, the

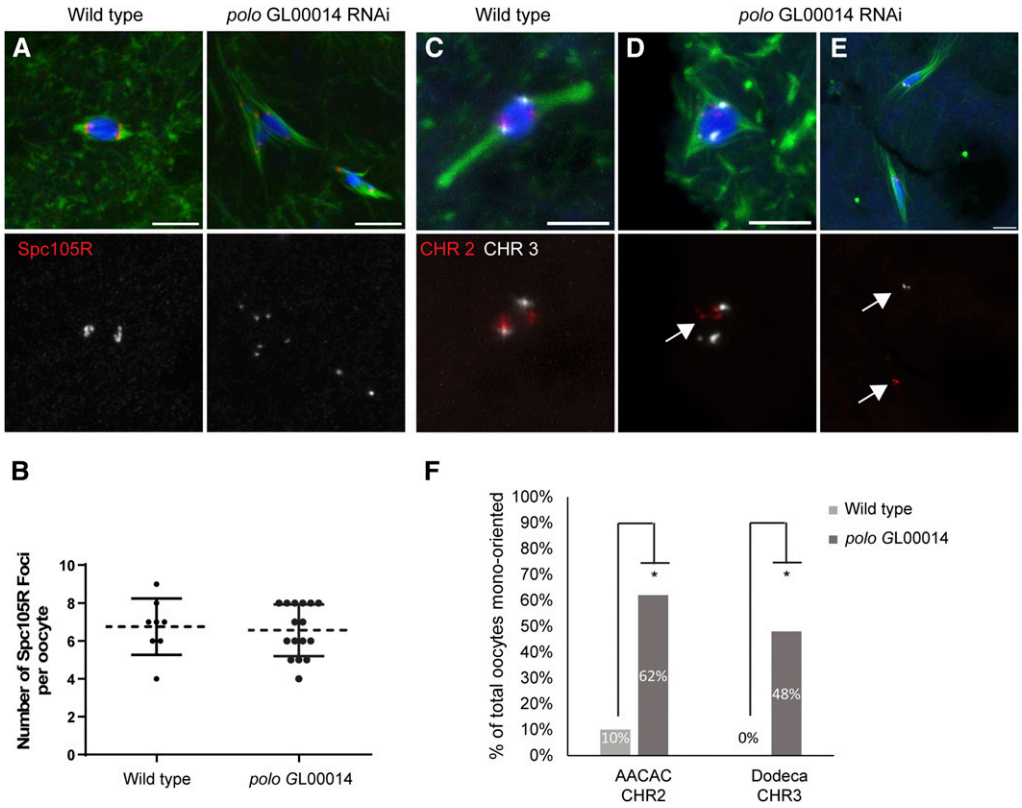

Figure 2 Polo is required for bi-orientation but not kinetochore protein localization. (A) Wild-type and *polo* RNAi oocytes were stained with SPC105R antibody to examine localization of kinetochore components. SPC105R is in red, DNA in blue, and tubulin in green while the single channel shows SPC105R in white. (B) Graph showing the number of SPC105R foci in wild-type and *polo* GL00014 RNAi oocytes is not significantly different. (C–E) Probes to the AACAC repeat on the second chromosome (red) and the Dodeca satellite on the third chromosome (white) were used to assess bi-orientation. (C) In wild-type oocytes the second and third chromosomes bi-orient toward the two poles within a single karyosome. (D and E) *polo* RNAi oocytes showing mono-orientation (arrows) without and with a karyosome defect, respectively. Bars, 5 μm. (F) Summary of orientation defects in wild-type and *polo* GL00014 RNAi oocytes. Asterisk shows significantly higher mono-orientation compared to wild type. *P*-values are in Table 3.

chromosomes were clustered with their centromeres oriented toward the two poles while the central spindle proteins like Subito and Incenp localize in a ring around the karyosome (Figure 3B). In oocytes depleted of *tum* by heat-shock-induced RNAi, Subito was mislocalized over the entire spindle (65%; $n = 20$; $P < <0.05$) instead of its normal restriction to the central spindle in wild type ($n = 14$) (Figure 3C). Since TUM localization is abnormal in *sub* mutants (Jang *et al.* 2005), these results indicate that Subito and TUM are interdependent for their localization during meiosis. TUM-depleted spindles also had frayed microtubules or polarity defects (70%; $n = 20$; $P < <0.05$) as compared to wild type (14%; $n = 14$) (Figure 3, D and E). These oocytes frequently had grossly elongated or broken karyosomes (Figure 3F) (47%; $n = 45$; $P < 0.0004$) compared to wild-type oocytes (9%; $n = 33$).

Defects in spindle assembly can lead to mono-orientation, where homologous centromeres are oriented toward the same pole. To test if *tum* knockdown oocytes had bi-orientation defects, we performed FISH with probes to the heterochromatic regions of the second (AACAC repeat) and third (Dodeca satellite repeat) chromosomes. We found that in *tum* knockdown oocytes, 50% of oocytes had AACAC mono-oriented ($n = 20$; $P < 0.05$) and 45% of oocytes had Dodeca mono-oriented ($n = 20$; $P < 0.05$) as compared to 5.5% in wild type ($n = 18$) (Figure 3, F and G; Table 3). These results show that TUM is required for meiotic spindle assembly and chromosome bi-orientation.

Meiotic function of Centralspindlin may depend on Rho1 activation

Since the above results show that the Centralspindlin complex is required for meiotic chromosome segregation, we investigated the role of the proteins activated by this complex. Pebble, a Rho Guanine Exchange Factor (GEF, ECT2 homolog), associates with the Centralspindlin complex during mitotic anaphase, and together they regulate the GTPase Rho1 (RhoA) and its downstream effectors such as Citron kinase (encoded by *sticky*) (O'Keefe *et al.* 2001; Somers and Saint 2003; Yüce *et al.* 2005). There is also a second GEF, RhoGEF2, that may play a role in the germline (Padash Barmchi *et al.* 2005). Rho1 and Sticky (citron kinase homolog) are recruited by Centralspindlin to the spindle midzone during mitosis (D'Avino *et al.* 2004; Bassi *et al.* 2011, 2013). We failed to detect localization of Rho1 to the meiotic spindle using available antibodies. However, these negative results could be explained by localization to membranes, the actin cytoskeleton, or that some antibodies are very sensitive to fixation conditions in *Drosophila* oocytes (McKim *et al.* 2009). In contrast, we did detect Sticky on oocyte meiotic spindles (Figure S9).

To examine their roles in spindle microtubule organization and homologous chromosome bi-orientation in oocytes, *matalpha4-GAL-VP16}V37* was used to express shRNAs against *Rho1*, *sticky*, *RhoGEF2*, and *pebble* (HMS00375, GL00312,

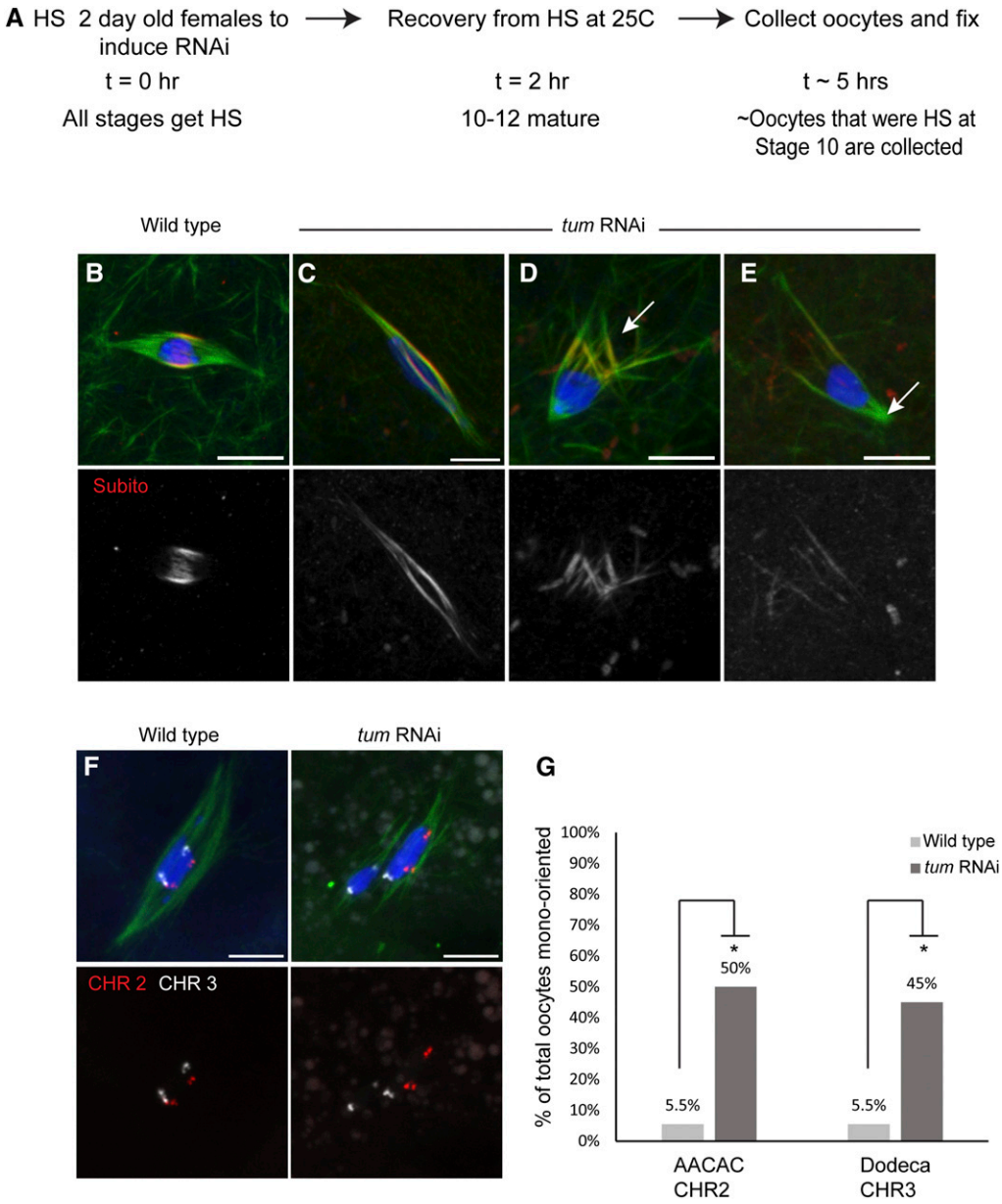

Figure 3 TUM is required for proper localization of Subito to the central spindle and chromosome segregation during meiosis I. (A) Protocol used to induce RNAi expression late in oogenesis to bypass the early requirement of TUM in oocyte development. The heat-shock treatment caused some mild karyosome defects in the controls. However, these were occasionally observed in wild type, and the mutant defects were qualitatively different because they involved spindle organization defects not observed in the controls. (B–E) Wild-type and *tum* RNAi females were heat-shocked and examined for central spindle components. DNA is shown in blue, tubulin in green, and Subito in red in merged images. (B) Subito localizes to the central spindle region in wild type. (C–E) *tum* RNAi oocytes showing diffuse Subito staining all along the length of the spindle (C); frayed spindles are in D, and monopolar spindles are in E. (F) Wild-type and *tum* RNAi oocytes showing FISH probes AACAC (chromosome 2) in red and Dodeca (chromosome 3) in white. (G) Summary of mono-orientation frequency in *tum* RNAi oocytes compared to wild type. Asterisk indicates significantly different values. *P*-values are calculated by Fisher's exact test (Table 3). Bars, 5 μm.

HMS01118, and GL01092, respectively). Expression of each shRNA with *P{tubP-GAL4}LL7* caused lethality, suggesting that the proteins were indeed knocked down. Consistent with this, all four shRNAs caused significant knockdowns when evaluated using qRT-PCR of oocytes (Table S2).

We used antibodies against Subito and INCENP as markers for the integrity of the meiotic central spindle. Wild-type metaphase spindles have a well-defined band of Subito and INCENP and a bipolar spindle ($n = 30$) (Figure 4, A and F). However, *Rho1* RNAi oocytes showed a significantly higher level of abnormal spindle microtubule organization (40%, $P < <0.05$) accompanied by aberrant central spindle protein localization (Figure 4, B and F; Table S2). *Sticky* RNAi oocytes also showed significant microtubule disorganization (30%; $P < <0.05$) and Subito and INCENP mis-localization compared to wild-type control oocytes (Figure 4, C and F; Table S2). *RhoGEF2* and *pbl* RNAi oocytes did not show any significant defects in either spindle formation or Subito or INCENP localization (Figure 4, D–F; Table S2). These results indicate that some mitotic cytokinesis proteins regulate acentrosomal spindle assembly and central spindle integrity in meiosis.

To test whether *Rho1*, *sticky*, *RhoGEF2*, and *pebble* RNAi oocytes show bi-orientation defects, we performed FISH on knockdown oocytes. *Rho1*, *sticky*, and *RhoGEF2* showed significantly higher frequency of oocytes with mono-orientation defects compared to wild-type oocytes (Figure 5, A–D and F). In contrast, *pbl* RNAi oocytes showed no AACAC or Dodeca mono-orientation defects ($n = 15$) (Figure 5, E and F; Table 3). These results indicate that Rho1, Sticky, and RhoGEF2, but not Pebble, are required for the kinetochores to make correct attachments to microtubules that result in bi-orientation.

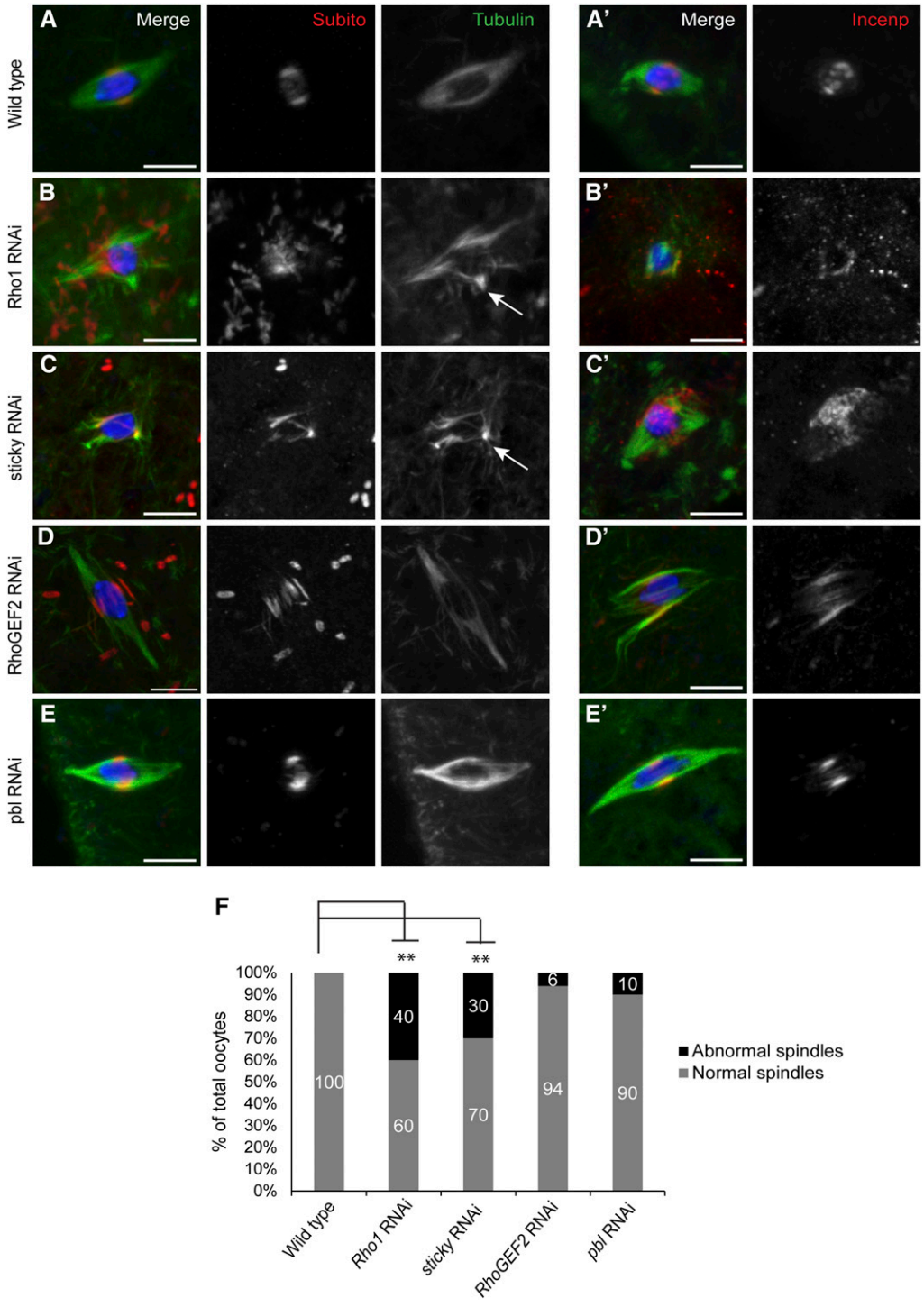

Figure 4 Mitotic midzone proteins affect microtubule organization and central spindle protein localization in meiotic metaphase I. Oocytes were stained with DNA (blue), Tubulin (green), and Subito or INCENP (red). (A and A′) Wild-type oocytes localize Subito or INCENP to the central region of a bipolar metaphase spindle. (B and B′) *Rho1* and (C and C′) *sticky* RNAi oocytes show disorganized microtubules (marked with arrows) and aberrant Subito or INCENP localization. (D and D′) *RhoGEF2* and (E and E′) *pbl* RNAi oocytes resemble wild type in both microtubule organization and Subito localization. (F) Graph summarizing the spindle defects in wild-type and RNAi oocytes. Significantly different *P*-values are indicated by asterisks. Bars, 5 μm.

Discussion

While the microtubules of the acentrosomal spindle may be nucleated from cytoplasmic MTOCs (Schuh and Ellenberg 2007) or from the chromatin itself (Heald *et al.* 1996), additional factors are required to organize them and segregate chromosomes. One such factor is the kinesin-6 motor protein Subito, which functions in cytokinesis during mitotic anaphase, but during acentrosomal meiosis it is required to organize a bipolar spindle (Giunta *et al.* 2002). Similarly, another prominent central spindle component is the CPC, which is also required for acentrosomal spindle assembly (Colombié *et al.* 2008; Radford *et al.* 2012). Based on these and other studies, we and others have suggested that, in the absence of centrosomes, the central spindle has a critical role in organizing the microtubules and chromosome alignment (Jang *et al.* 2005; Resnick *et al.* 2006; Dumont and Desai 2012; Radford *et al.* 2012). Thus, we have initiated

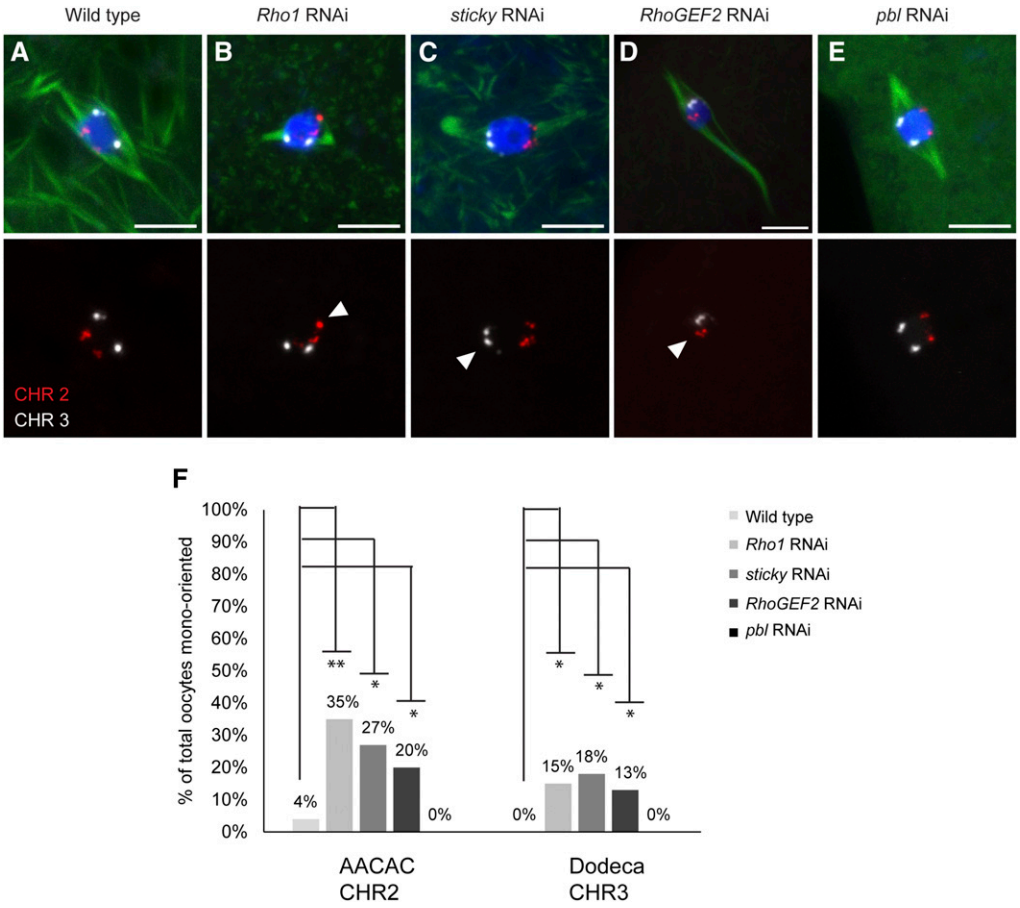

Figure 5 Homologous chromosome bi-orientation is affected by *Rho1*, *sticky*, and *RhoGEF2* but not by *pbl* RNAi. (A–E) (Top) Merged images with FISH probes AACAC (chromosome 2) in red and Dodeca (chromosome 3) in white. DNA is in blue and tubulin is in green. (A) The probes in wild type are bi-oriented toward the two poles. (B–D) *Rho1*, *sticky*, and *RhoGEF2* RNAi oocytes show one or both probes mono-oriented. (E) *pbl* RNAi oocyte with no orientation defect. (Bottom) Only the probes are shown, with mono-orientation marked by arrowheads. Bars, 5 μm. (F) Summary of orientation defects. Significantly higher mono-orientation defects in mutants are indicated by asterisks, and *P*-values are indicated in Table 3.

the first comprehensive study of central spindle protein function in acentrosomal spindle assembly and chromosome segregation.

Cytological analysis of mitotic cells has shown that Subito is required to localize the CPC to the midzone during cytokinesis (Cesario *et al.* 2006), consistent with the studies of its human homolog, MKLP2 (Gruneberg *et al.* 2004). This function becomes only essential when the dosage of the CPC is reduced. We have used this observation to identify genes that interact genetically with *sub*, with the expectation that we might find other genes that function in meiotic spindle assembly like the CPC and Subito. We identified proteins associated with the mitotic central spindle or midzone, such as all CPC and Centralspindlin components. Furthermore, we confirmed that several mitotic central spindle genes have a role in meiotic acentrosomal spindle assembly. These are functions during metaphase I, rather than anaphase and cytokinesis as in mitotic cells. Finally, this study has identified at least 16 novel loci that interact with *sub* (synthetic lethal) and at least six novel loci on the third chromosome that interact meiotically with *Incenp*.

Polo may function only at the kinetochore during female metaphase I

We had previously found that *polo* mutations cause synthetic lethality and that there is a direct interaction between Polo and Subito (Cesario *et al.* 2006). Therefore, we determined if Polo has a meiotic central spindle function. Previous work in *Drosophila* has shown that Polo inhibition by Matrimony is important for maintaining prophase arrest (Xiang *et al.* 2007; Bonner *et al.* 2013), but its role in meiosis I has not been characterized. Polo has diverse roles in mitosis ranging from centrosome maturation, spindle assembly, kinetochore attachment, the SAC response, and cytokinesis (Carmena *et al.* 1998; Petronczki *et al.* 2008). Correlating with these diverse functions, Polo localizes to the centrosomes and centromeres at metaphase and the midzone at anaphase. Meiotic metaphase is different, however, because Polo retains its localization to the centromeres (Jang *et al.* 2005), unlike meiotic central spindle proteins like Subito and the CPC. In analyzing oocytes lacking Polo, we observed two prominent phenotypes. First, the chromosomes were disorganized, resulting in the failure to maintain a single karyosome. Second, these oocytes form aberrant spindles that appear to be composed mostly of central spindle. The spindles often appear "hollow," which can reflect loss of kinetochore but not central spindle microtubules (Radford *et al.* 2015). These results are consistent with a role for Polo in stabilizing microtubule–kinetochore attachments (Elowe *et al.* 2007; Lénárt *et al.* 2007; Liu *et al.* 2012; Suijkerbuijk *et al.* 2012) but with no function in the central spindle. These results also show that, while the meiotic metaphase central spindle contains many proteins found in the anaphase midzone, it also has important

differences. Indeed, it remains to be determine if Polo relocalizes to the midzone at anaphase I.

Mitotic spindle midzone proteins regulate acentrosomal spindle function

From our genetic screens, we identified mutations in all the components of two essential mitotic central spindle components: the CPC and Centralspindlin. Our analysis of TUM shows that Centralspindlin also plays an important role in organizing the acentrosomal spindle and localizing Subito. It is possible that, since Centralspindlin colocalizes with Subito in meiosis, it is involved in stabilizing the interpolar microtubules in the central spindle. TUM localization is in turn dependent on Subito, demonstrating the underlying interdependence of the meiotic central spindle proteins (Jang *et al.* 2005).

In its cytokinesis role, Centralspindlin signals to the actomyosin complex via the RhoA pathway. Pebble, the *Drosophila* homolog of GEF ECT2, is critical for cytokinesis (Yüce *et al.* 2005; Simon *et al.* 2008; Wolfe *et al.* 2009), interacts with RacGAP50C (O'Keefe *et al.* 2001; Somers and Saint 2003), and activates RhoA. Indeed, we found that Centralspindlin downstream effectors Rho1 (RhoA) and Sticky (Citron kinase) are required for accurate meiotic chromosome segregation. Loss of these proteins resulted in spindle assembly and centromere bi-orientation defects. This is the first report that the contractile ring proteins have been shown to be involved in meiotic chromosome segregation. Given these results, however, it was surprising that Pebble was not found to be critical for meiosis. *Drosophila*, however, has RhoGEF2 that is also a GEF and is required to regulate actin organization and contractility in the embryo (Padash Barmchi *et al.* 2005).

A hierarchy of central spindle assembly and function

None of the knockdowns we have studied have the same phenotype as a *sub* mutant with spindle bipolarity defects. Similarly, while we identified several interesting genes that interact with *Incenp*, most did not interact as strongly as *sub* mutants. We suggest that this interaction occurs because the epitope tag fused to the N terminus of the *Incenp* allele causes the dominant phenotype, and there is a direct physical interaction between Subito and the N terminus of INCENP, as recently described for MKLP2 (Kitagawa *et al.* 2014). That we observed consistent genetic interactions between *Incenp* and Cyclin B and some of its regulators, which are also known to regulate Subito/Mklp2 localization (Hummer and Mayer 2009; Kitagawa *et al.* 2014), is consistent with a specific direct interaction between Subito and Incenp. A surprisingly strong interaction was also observed between *Incenp* and *ncd* mutants, suggesting that the NCD motor has an important role in central spindle assembly. Indeed, we previously observed an allele-specific genetic interaction between *ncd* and *sub* (Giunta *et al.* 2002). These results are striking because *ncd* mutants do not have cytokinesis defects, suggesting that NCD may have a specific function in the central spindle of acentrosomal meiosis.

Based on the lack of mutants with phenotypes similar to *sub*, we suggest that the integrity of the meiotic central spindle and spindle bipolarity may depend only on the activity of Subito to bundle antiparallel microtubules. Our results also show, however, that contractile ring proteins are required in meiosis to maintain the organization of microtubules and promote homolog bi-orientation. One interpretation of these data is that the actin cytoskeleton is required for the organization or function of the meiotic central spindle microtubules. While the actin cytoskeleton is required to position the meiotic spindle in some systems (Brunet and Verlhac 2011; Fabritius *et al.* 2011; McNally 2013), it could also affect functioning of the spindle itself. Indeed, the formin mDIA3 has been shown to be involved in recruiting Aurora B for error correction (Mao 2011). RhoA has been shown to regulate microtubule stability, possibly through its downstream effectors mDia or Tau (Cook *et al.* 1998; Waterman-Storer *et al.* 2000; Palazzo *et al.* 2001). In the future, it will be important to directly perturb the actin cytoskeleton and examine chromosome alignment and segregation.

An alternative is that the contractile ring proteins directly regulate microtubule organization. Interestingly, RhoGEF2 has been found to associate with microtubule plus ends in a process that depends on EB1 (Rogers *et al.* 2004). Citron kinase (Sticky), rather than functioning simply as a downstream effector of RhoA, directly interacts with Pavarotti and another Kinesin, Nebbish (Klp38B), and is required for RhoA and Pavarotti localization and midzone formation (Bassi *et al.* 2011, 2013). In the future, it will be important to determine if the meiotic function of Citron kinase depends on interactions with actomyosin components or only with the microtubules.

Our results implicate proteins required during mitosis for midzone function and cytokinesis in meiotic chromosome segregation. In cytokinesis, a precise position of a division plane must be established (D'Avino *et al.* 2015). This activity may also be important for the acentrosomal spindle; a precise division plane may be established during metaphase I to sort each pair of homologous chromosomes. This process could result in the two kinetochores of each bivalent interacting with the microtubules from opposite poles. Activities such as those promoted by the Centralspindlin complex may fine-tune the central spindle structure to create a precise division plane. Further studies will be required, however, to determine if the meiotic spindle depends on interactions with the actin cytoskeleton for chromosome segregation or if these proteins exert their effects only through central spindle microtubules at meiosis I.

Acknowledgments

We thank Li Nguyen for technical assistance; Karen Schindler, Ruth Steward, and members of the McKim lab for helpful comments on the manuscript; Christian Lehner, David Glover, and Robert Saint for providing antibodies; and the Transgenic RNAi Project at Harvard Medical School

[National Institutes of Health (NIH)/*National Institute of General Medical Sciences* grant R01-GM084947] for providing transgenic RNAi fly stocks. Fly stocks obtained from the Bloomington *Drosophila* Stock Center (NIH grant P40OD018537) were also used in this study. A.D. was funded by a Busch Predoctoral Fellowship, and S.J.S., B.F., and R.A.B. were funded by an Aresty Foundation Summer Research Fellowship. This work was supported by NIH grant GM101955 (to K.S.M.).

Literature Cited

Adams, R. R., A. A. Tavares, A. Salzberg, H. J. Bellen, and D. M. Glover, 1998 pavarotti encodes a kinesin-like protein required to organize the central spindle and contractile ring for cytokinesis. Genes Dev. 12: 1483–1494.

Ashraf, S. I., and Y. T. Ip, 2001 The Snail protein family regulates neuroblast expression of inscuteable and string, genes involved in asymmetry and cell division in Drosophila. Development 128: 4757–4767.

Ashraf, S. I., X. Hu, J. Roote, and Y. T. Ip, 1999 The mesoderm determinant snail collaborates with related zinc-finger proteins to control Drosophila neurogenesis. EMBO J. 18: 6426–6438.

Bassi, Z. I., K. J. Verbrugghe, L. Capalbo, S. Gregory, E. Montembault *et al.*, 2011 Sticky/Citron kinase maintains proper RhoA localization at the cleavage site during cytokinesis. J. Cell Biol. 195: 595–603.

Bassi, Z. I., M. Audusseau, M. G. Riparbelli, G. Callaini, and P. P. D'Avino, 2013 Citron kinase controls a molecular network required for midbody formation in cytokinesis. Proc. Natl. Acad. Sci. USA 110: 9782–9787.

Bonner, A. M., S. E. Hughes, J. A. Chisholm, S. K. Smith, B. D. Slaughter *et al.*, 2013 Binding of Drosophila Polo kinase to its regulator Matrimony is noncanonical and involves two separate functional domains. Proc. Natl. Acad. Sci. USA 110: E1222–E1231.

Brunet, S., and M. H. Verlhac, 2011 Positioning to get out of meiosis: the asymmetry of division. Hum. Reprod. Update 17: 68–75.

Callaini, G., and M. G. Riparbelli, 1996 Fertilization in Drosophila melanogaster: centrosome inheritance and organization of the first mitotic spindle. Dev. Biol. 176: 199–208.

Carmena, M., M. G. Riparbelli, G. Minestrini, A. M. Tavares, R. Adams *et al.*, 1998 Drosophila polo kinase is required for cytokinesis. J. Cell Biol. 143: 659–671.

Cesario, J. M., J. K. Jang, B. Redding, N. Shah, T. Rahman *et al.*, 2006 Kinesin 6 family member Subito participates in mitotic spindle assembly and interacts with mitotic regulators. J. Cell Sci. 119: 4770–4780.

Chou, T. B., and N. Perrimon, 1996 The autosomal FLP-DFS technique for generating germline mosaics in *Drosophila melanogaster*. Genetics 144: 1673–1679.

Colombié, N., C. F. Cullen, A. L. Brittle, J. K. Jang, W. C. Earnshaw *et al.*, 2008 Dual roles of Incenp crucial to the assembly of the acentrosomal metaphase spindle in female meiosis. Development 135: 3239–3246.

Cook, T. A., T. Nagasaki, and G. G. Gundersen, 1998 Rho guanosine triphosphatase mediates the selective stabilization of microtubules induced by lysophosphatidic acid. J. Cell Biol. 141: 175–185.

D'Avino, P. P., M. S. Savoian, and D. M. Glover, 2004 Mutations in sticky lead to defective organization of the contractile ring during cytokinesis and are enhanced by Rho and suppressed by Rac. J. Cell Biol. 166: 61–71.

D'Avino, P. P., M. S. Savoian, L. Capalbo, and D. M. Glover, 2006 RacGAP50C is sufficient to signal cleavage furrow formation during cytokinesis. J. Cell Sci. 119: 4402–4408.

D'Avino, P. P., M. G. Giansanti, and M. Petronczki, 2015 Cytokinesis in animal cells. Cold Spring Harb. Perspect. Biol. 7: a015834.

Doubilet, S., and K. S. McKim, 2007 Spindle assembly in the oocytes of mouse and Drosophila: similar solutions to a problem. Chromosome Res. 15: 681–696.

Dumont, J., and A. Desai, 2012 Acentrosomal spindle assembly and chromosome segregation during oocyte meiosis. Trends Cell Biol. 22: 241–249.

Elowe, S., S. Hümmer, A. Uldschmid, X. Li, and E. A. Nigg, 2007 Tension-sensitive Plk1 phosphorylation on BubR1 regulates the stability of kinetochore microtubule interactions. Genes Dev. 21: 2205–2219.

Fabritius, A. S., M. L. Ellefson, and F. J. McNally, 2011 Nuclear and spindle positioning during oocyte meiosis. Curr. Opin. Cell Biol. 23: 78–84.

Fededa, J. P., and D. W. Gerlich, 2012 Molecular control of animal cell cytokinesis. Nat. Cell Biol. 14: 440–447.

Giunta, K. L., J. K. Jang, E. A. Manheim, G. Subramanian, and K. S. McKim, 2002 subito encodes a kinesin-like protein required for meiotic spindle pole formation in *Drosophila melanogaster*. Genetics 160: 1489–1501.

Gloor, G. B., C. R. Preston, D. M. Johnson-Schlitz, N. A. Nassif, R. W. Phillis *et al.*, 1993 Type I repressors of *P* element mobility. Genetics 135: 81–95.

Glotzer, M., 2005 The molecular requirements for cytokinesis. Science 307: 1735–1739.

Goldstein, A. Y., Y. N. Jan, and L. Luo, 2005 Function and regulation of Tumbleweed (RacGAP50C) in neuroblast proliferation and neuronal morphogenesis. Proc. Natl. Acad. Sci. USA 102: 3834–3839.

Gruneberg, U., R. Neef, R. Honda, E. A. Nigg, and F. A. Barr, 2004 Relocation of Aurora B from centromeres to the central spindle at the metaphase to anaphase transition requires MKlp2. J. Cell Biol. 166: 167–172.

Gunsalus, K. C., S. Bonaccorsi, E. Williams, F. Verni, M. Gatti *et al.*, 1995 Mutations in twinstar, a Drosophila gene encoding a cofilin/ADF homologue, result in defects in centrosome migration and cytokinesis. J. Cell Biol. 131: 1243–1259.

Guse, A., M. Mishima, and M. Glotzer, 2005 Phosphorylation of ZEN-4/MKLP1 by aurora B regulates completion of cytokinesis. Curr. Biol. 15: 778–786.

Heald, R., R. Tournebize, T. Blank, R. Sandaltzopoulos, P. Becker *et al.*, 1996 Self-organization of microtubules into bipolar spindles around artificial chromosomes in Xenopus egg extracts. Nature 382: 420–425.

Herbert, M., D. Kalleas, D. Cooney, M. Lamb, and L. Lister, 2015 Meiosis and maternal aging: insights from aneuploid oocytes and trisomy births. Cold Spring Harb. Perspect. Biol. 7: a017970.

Hummer, S., and T. U. Mayer, 2009 Cdk1 negatively regulates midzone localization of the mitotic kinesin Mklp2 and the chromosomal passenger complex. Curr. Biol. 19: 607–612.

Jang, J. K., T. Rahman, and K. S. McKim, 2005 The kinesinlike protein Subito contributes to central spindle assembly and organization of the meiotic spindle in Drosophila oocytes. Mol. Biol. Cell 16: 4684–4694.

Kim, J., K. Ishiguro, A. Nambu, B. Akiyoshi, S. Yokobayashi *et al.*, 2015 Meikin is a conserved regulator of meiosis-I-specific kinetochore function. Nature 517: 466–471.

Kitagawa, M., S. Y. Fung, U. F. Hameed, H. Goto, M. Inagaki *et al.*, 2014 Cdk1 coordinates timely activation of MKlp2 kinesin with relocation of the chromosome passenger complex for cytokinesis. Cell Reports 7: 166–179.

Lai, S. L., M. R. Miller, K. J. Robinson, and C. Q. Doe, 2012 The Snail family member Worniu is continuously required in neuroblasts to prevent Elav-induced premature differentiation. Dev. Cell 23: 849–857.

Liu, D., O. Davydenko, and M. A. Lampson, 2012 Polo-like kinase-1 regulates kinetochore-microtubule dynamics and spindle checkpoint silencing. J. Cell Biol. 198: 491–499.

Lénárt, P., M. Petronczki, M. Steegmaier, B. Di Fiore, J. J. Lipp *et al.*, 2007 The small-molecule inhibitor BI 2536 reveals novel insights into mitotic roles of polo-like kinase 1. Curr. Biol. 17: 304–315.

Magie, C. R., D. Pinto-Santini, and S. M. Parkhurst, 2002 Rho1 interacts with p120ctn and alpha-catenin, and regulates cadherin-based adherens junction components in Drosophila. Development 129: 3771–3782.

Mao, Y., 2011 FORMIN a link between kinetochores and microtubule ends. Trends Cell Biol. 21: 625–629.

Matthies, H. J., H. B. McDonald, L. S. Goldstein, and W. E. Theurkauf, 1996 Anastral meiotic spindle morphogenesis: role of the non-claret disjunctional kinesin-like protein. J. Cell Biol. 134: 455–464.

McKim, K. S., E. F. Joyce, and J. K. Jang, 2009 Cytological analysis of meiosis in fixed Drosophila ovaries. Methods Mol. Biol. 558: 197–216.

McNally, F. J., 2013 Mechanisms of spindle positioning. J. Cell Biol. 200: 131–140.

Minestrini, G., A. S. Harley, and D. M. Glover, 2003 Localization of Pavarotti-KLP in living Drosophila embryos suggests roles in reorganizing the cortical cytoskeleton during the mitotic cycle. Mol. Biol. Cell 14: 4028–4038.

Musacchio, A., and E. D. Salmon, 2007 The spindle-assembly checkpoint in space and time. Nat. Rev. Mol. Cell Biol. 8: 379–393.

Neef, R., C. Preisinger, J. Sutcliffe, R. Kopajtich, E. A. Nigg *et al.*, 2003 Phosphorylation of mitotic kinesin-like protein 2 by polo-like kinase 1 is required for cytokinesis. J. Cell Biol. 162: 863–875.

Ni, J. Q., R. Zhou, B. Czech, L. P. Liu, L. Holderbaum *et al.*, 2011 A genome-scale shRNA resource for transgenic RNAi in Drosophila. Nat. Methods 8: 405–407.

O'Keefe, L., W. G. Somers, A. Harley, and R. Saint, 2001 The pebble GTP exchange factor and the control of cytokinesis. Cell Struct. Funct. 26: 619–626.

Padash Barmchi, M., S. Rogers, and U. Häcker, 2005 DRhoGEF2 regulates actin organization and contractility in the Drosophila blastoderm embryo. J. Cell Biol. 168: 575–585.

Palazzo, A. F., T. A. Cook, A. S. Alberts, and G. G. Gundersen, 2001 mDia mediates Rho-regulated formation and orientation of stable microtubules. Nat. Cell Biol. 3: 723–729.

Pavicic-Kaltenbrunner, V., M. Mishima, and M. Glotzer, 2007 Cooperative assembly of CYK-4/MgcRacGAP and ZEN-4/MKLP1 to form the centralspindlin complex. Mol. Biol. Cell 18: 4992–5003.

Petronczki, M., P. Lénárt, and J. M. Peters, 2008 Polo on the rise: from mitotic entry to cytokinesis with Plk1. Dev. Cell 14: 646–659.

Polevoy, G., H. C. Wei, R. Wong, Z. Szentpetery, Y. J. Kim *et al.*, 2009 Dual roles for the Drosophila PI 4-kinase four wheel drive in localizing Rab11 during cytokinesis. J. Cell Biol. 187: 847–858.

Radford, S. J., J. K. Jang, and K. S. McKim, 2012 The chromosomal passenger complex is required for meiotic acentrosomal spindle assembly and chromosome bi-orientation. Genetics 192: 417–429.

Radford, S. J., T. L. Hoang, A. A. Głuszek, H. Ohkura, and K. S. McKim, 2015 Lateral and end-on kinetochore attachments are coordinated to achieve bi-orientation in Drosophila oocytes. PLoS Genet. 11: e1005605.

Resnick, T. D., D. L. Satinover, F. MacIsaac, P. T. Stukenberg, W. C. Earnshaw *et al.*, 2006 INCENP and Aurora B promote meiotic sister chromatid cohesion through localization of the Shugoshin MEI-S332 in Drosophila. Dev. Cell 11: 57–68.

Riparbelli, M. G., and G. Callaini, 2005 The meiotic spindle of the Drosophila oocyte: the role of centrosomin and the central aster. J. Cell Sci. 118: 2827–2836.

Rogers, S. L., U. Wiedemann, U. Häcker, C. Turck, and R. D. Vale, 2004 Drosophila RhoGEF2 associates with microtubule plus ends in an EB1-dependent manner. Curr. Biol. 14: 1827–1833.

Rorth, P., 1998 Gal4 in the Drosophila female germline. Mech. Dev. 78: 113–118.

Ruchaud, S., M. Carmena, and W. C. Earnshaw, 2007 Chromosomal passengers: conducting cell division. Nat. Rev. Mol. Cell Biol. 8: 798–812.

Schittenhelm, R. B., S. Heeger, F. Althoff, A. Walter, S. Heidmann *et al.*, 2007 Spatial organization of a ubiquitous eukaryotic kinetochore protein network in Drosophila chromosomes. Chromosoma 116: 385–402.

Schittenhelm, R. B., R. Chaleckis, and C. F. Lehner, 2009 Intrakinetochore localization and essential functional domains of Drosophila Spc105. EMBO J. 28: 2374–2386.

Schuh, M., and J. Ellenberg, 2007 Self-organization of MTOCs replaces centrosome function during acentrosomal spindle assembly in live mouse oocytes. Cell 130: 484–498.

Simon, G. C., E. Schonteich, C. C. Wu, A. Piekny, D. Ekiert *et al.*, 2008 Sequential Cyk-4 binding to ECT2 and FIP3 regulates cleavage furrow ingression and abscission during cytokinesis. EMBO J. 27: 1791–1803.

Somers, W. G., and R. Saint, 2003 A RhoGEF and Rho family GTPase-activating protein complex links the contractile ring to cortical microtubules at the onset of cytokinesis. Dev. Cell 4: 29–39.

Spradling, A. C., 1993 Developmental genetics of oogenesis, pp. 1–70 in *The Development of Drosophila melanogaster*, edited by M. Bate, and A. M. Arias. Cold Spring Harbor Laboratory Press, Cold Spring Harbor, NY.

Suijkerbuijk, S. J., M. Vleugel, A. Teixeira, and G. J. Kops, 2012 Integration of kinase and phosphatase activities by BUBR1 ensures formation of stable kinetochore-microtubule attachments. Dev. Cell 23: 745–755.

Theurkauf, W. E., and R. S. Hawley, 1992 Meiotic spindle assembly in Drosophila females: behavior of nonexchange chromosomes and the effects of mutations in the nod kinesin-like protein. J. Cell Biol. 116: 1167–1180.

Tseng, B. S., L. Tan, T. M. Kapoor, and H. Funabiki, 2010 Dual detection of chromosomes and microtubules by the chromosomal passenger complex drives spindle assembly. Dev. Cell 18: 903–912.

Waterman-Storer, C., D. Y. Duey, K. L. Weber, J. Keech, R. E. Cheney *et al.*, 2000 Microtubules remodel actomyosin networks in Xenopus egg extracts via two mechanisms of F-actin transport. J. Cell Biol. 150: 361–376.

Wolfe, B. A., T. Takaki, M. Petronczki, and M. Glotzer, 2009 Polo-like kinase 1 directs assembly of the HsCyk-4 RhoGAP/Ect2 RhoGEF complex to initiate cleavage furrow formation. PLoS Biol. 7: e1000110.

Xiang, Y., S. Takeo, L. Florens, S. E. Hughes, L. J. Huo *et al.*, 2007 The inhibition of polo kinase by matrimony maintains G2 arrest in the meiotic cell cycle. PLoS Biol. 5: e323.

Yüce, O., A. Piekny, and M. Glotzer, 2005 An ECT2-centralspindlin complex regulates the localization and function of RhoA. J. Cell Biol. 170: 571–582.

Zavortink, M., N. Contreras, T. Addy, A. Bejsovec, and R. Saint, 2005 Tum/RacGAP50C provides a critical link between anaphase microtubules and the assembly of the contractile ring in Drosophila melanogaster. J. Cell Sci. 118: 5381–5392.

Communicating editor: S. E. Bickel

GENETICS

Supporting Information
www.genetics.org/lookup/suppl/doi:10.1534/genetics.115.181081/-/DC1

Spindle Assembly and Chromosome Segregation Requires Central Spindle Proteins in *Drosophila* Oocytes

Arunika Das, Shital J. Shah, Bensen Fan, Daniel Paik, Daniel J. DiSanto, Anna Maria Hinman, Jeffry M. Cesario, Rachel A. Battaglia, Nicole Demos, and Kim S. McKim

DOI: 10.1534/genetics.115.181081

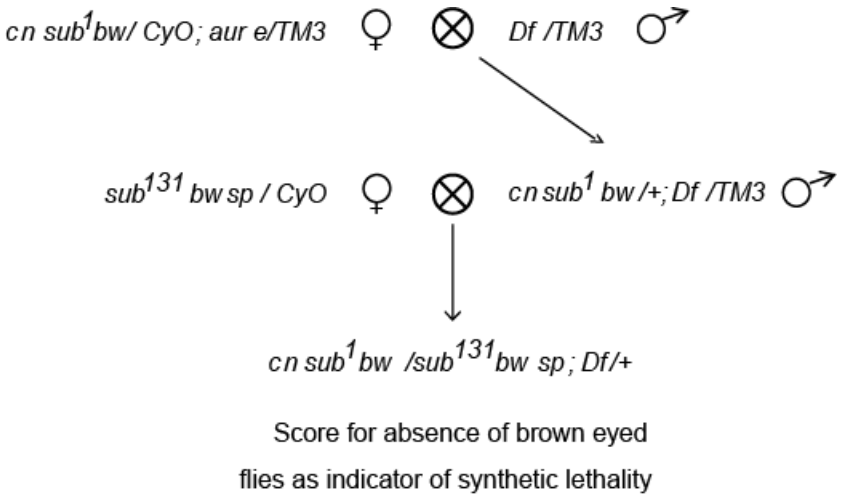

Figure S1: Synthetic lethal deficiency screen on the third chromosome.

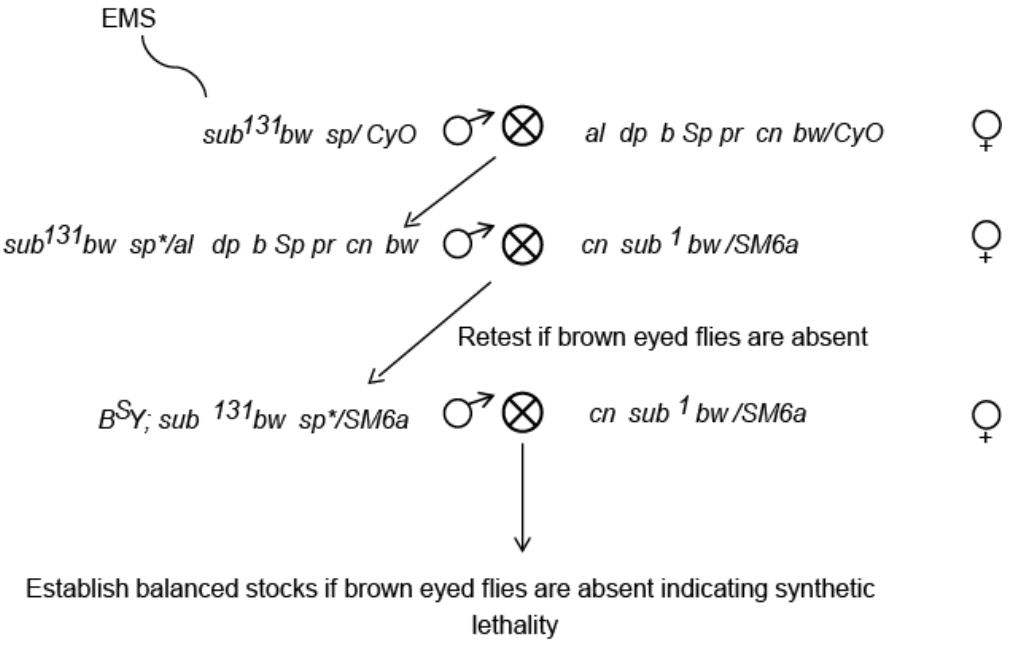

Figure S2: Synthetic lethal screen on the second chromosome. Crossing scheme for isolating heterozygous mutations that induce synthetic lethality in a *sub*^{131}*/sub*^{1} mutant. An asterisk indicates the EMS-treated chromosome. Synthetic lethality is assessed by the absence of straight winged, brown eyed flies in the second step and these mutations are further retested and balanced.

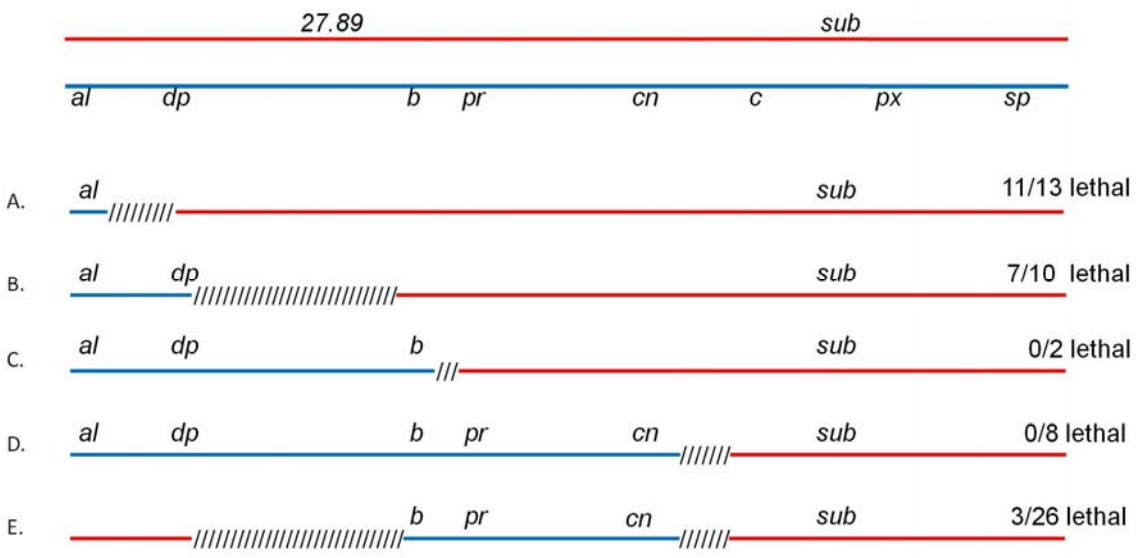

Figure S3: Genetic map showing the recombinants used for the mapping of *27.89*. The red lines represent the original mutagenized *27.89 sub*^{131} chromosome. The blue lines represent a chromosome with several recessive visible markers. The slash marks represent the possible area of crossing over for each recombinant. 13 of these crossed over between *al* and *dp*, and 11 of the 13 were synthetic lethal when crossed back to *sub*^{1}. There were 10 crossovers in between *dp* and *b*, of which 7 were synthetic lethal and thus had retained *27.89*. Two events crossed over between *b* and *pr* and neither of them retained *27.89*. Likewise, of the 8 that crossed over between *cn* and *c*, none displayed synthetic lethality. Finally, of the 26 double crossovers that crossed over once between *dp* and *b* and then again between *cn* and *c*, 3 had retained *27.89* and showed synthetic lethality.

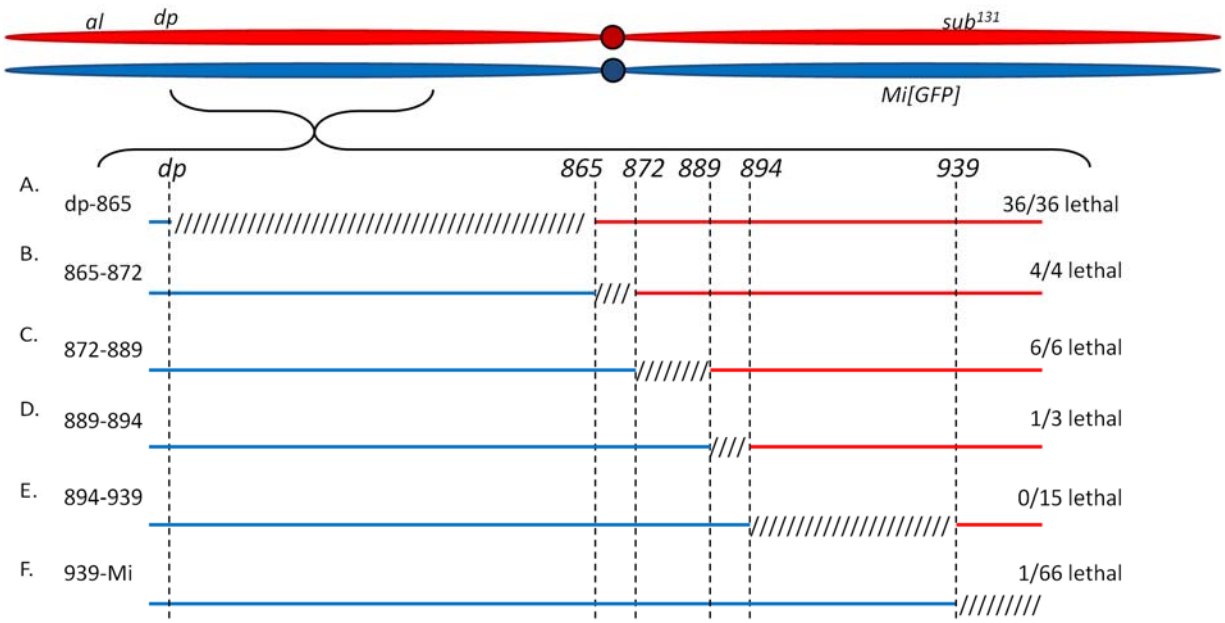

Figure S4: Schematic diagram of the recombinants used for Single Nucleotide Polymorphism marker mapping of *27.89*. Red lines represent the *27.89* mutant chromosome with the *al* and *dp* markers, *al dp 27.89 sub*^{131}. Blue lines represent a chromosome with many differing SNPs as well as a *Mi[GFP]* insertion just to the left of *subito*. The slash marks represent the possible area of crossing over for each recombinant. The locations of the individual SNP markers are indicated by the vertical dashed lines.

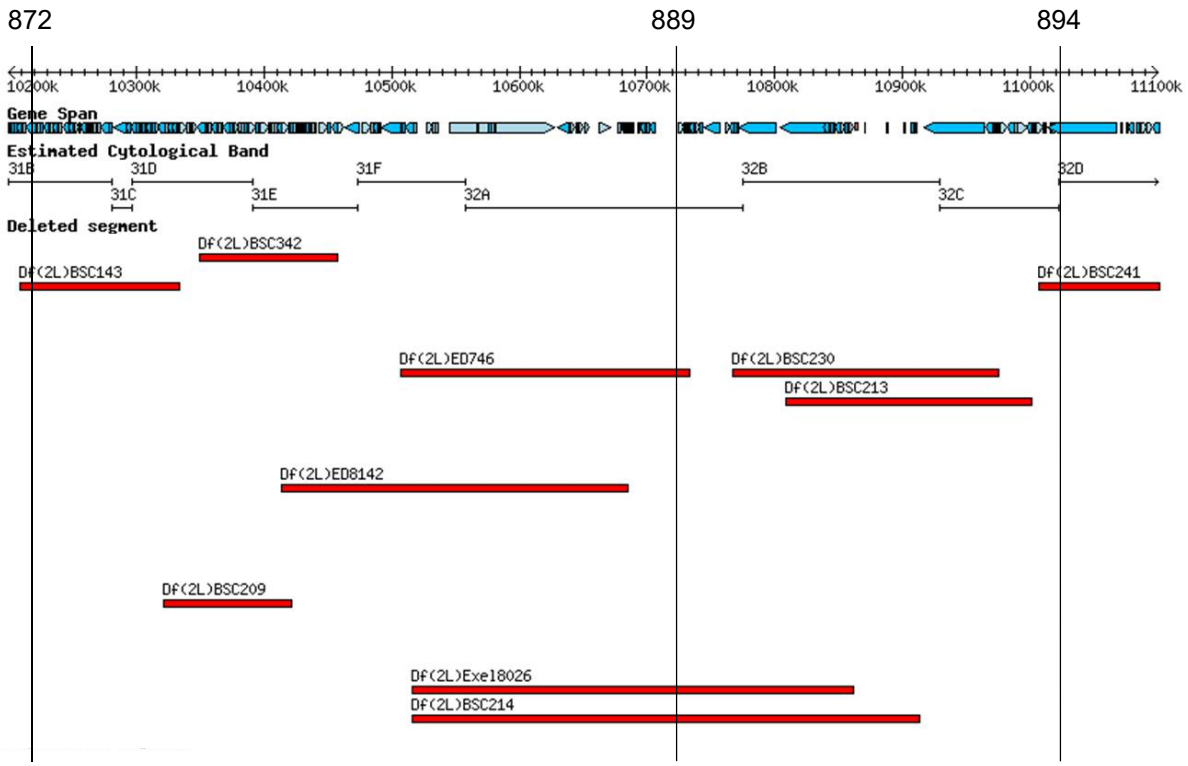

Figure S5: Schematic diagram of the chromosomal deletions used to deficiency map *27.89*. The red lines represent chromosomal deficiencies. The key SNP markers with which *27.89* was mapped are labeled at the top and delineated by the vertical black lines. Figure adapted from Flybase (GELBART *et al.* 1997).

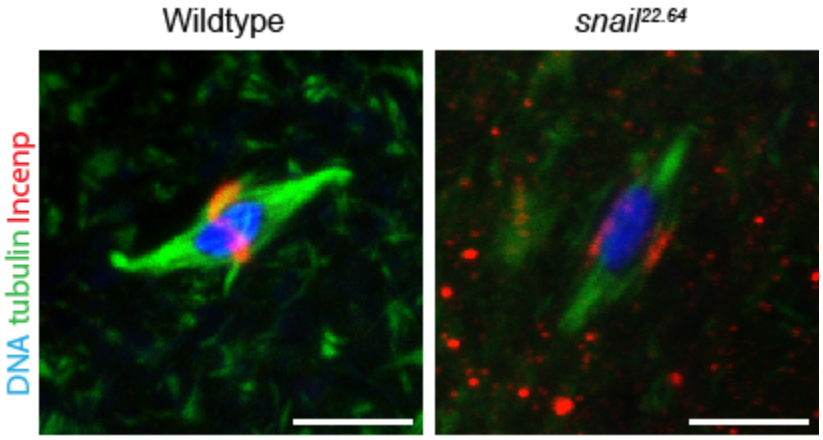

Figure S6: *snail*$^{22.64}$ mutant oocytes, (generated using germ line clones (CHOU and PERRIMON 1996) shows no effect on meiotic spindle assembly or central spindle localization. Wild-type or mutant oocytes were stained for DNA (blue), tubulin (green) and Incenp (red). Incenp (Inner centromere Protein) is a member of the CPC which localizes to the central spindle if formed correctly as shown here. Scale bars represent 5 μm.

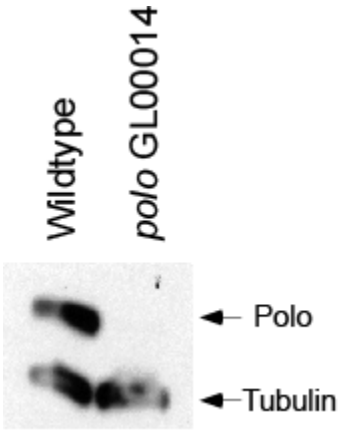

Figure S7: Western showing that the *polo* GL00014 hairpin does indeed knockdown POLO protein in the ovaries. POLO was detected using mouse monoclonal MA294 (LLAMAZARES *et al.* 1991) and Tubulin was used as a loading control.

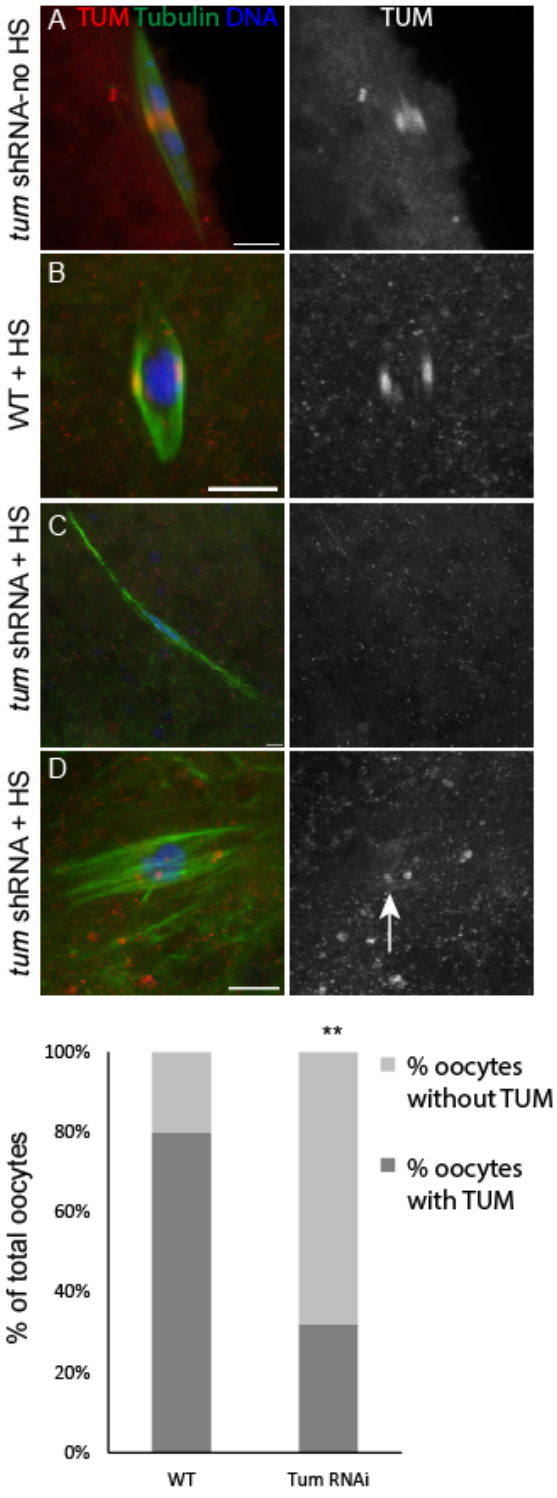

Figure S8: TUM knock down by heat shock induced RNAi. Oocytes are shown with TUM (red) to assess the level of knockdown following heat shock. Tubulin is in green and DNA is in blue. A-B) Both *tum* shRNA without heat shock and wild-type females with heat shock show TUM staining at the central spindle in almost all oocytes. C-D) TUM localization is greatly reduced or eliminated in oocytes. Faint staining (arrow) in some oocytes can be attributed to the non-uniformity of the heat shocked oocytes in adult females E) Quantification of TUM localization. The WT category includes both heat shocked and non-heat shocked oocytes; 80% of these oocytes had TUM localization to the spindle (n=24). In contrast, only 32% of *tum* RNAi oocytes had TUM localization, which is significantly lower than the controls, and was usually more diffuse and fainter than wild-type (n=28, Fisher's exact p-value =0.0012). The scale bars are 5 µm.

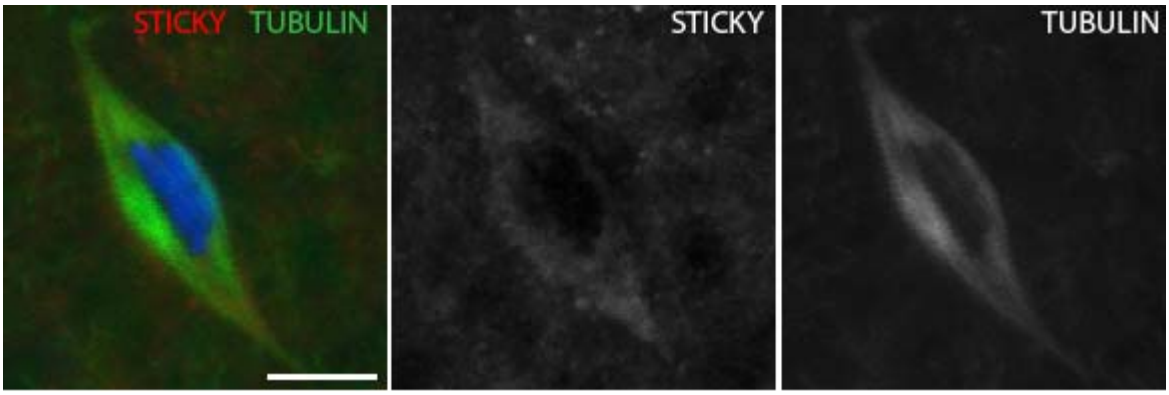

Figure S9: Sticky localizes to the meiotic spindle. Wild-type oocytes were stained with rabbit anti-Sticky antibody shown in red in merge and white in single channel. Tubulin is shown in green in the merge and white in single channel and DNA is in blue. The scale bar is 5 μm. We also tested a, but were unable to detect any localization.

Table S1: Mutations tested for dominant enhancement of *Incenp*^{myc}

Type/ Homolog	Mutant	Nondisjunction progeny	Total progeny	Nondisjuction (%)
Cell Cycle				
CDC2/CDK1	*Cdc2*$^{E1\text{-}24}$	28	1347	4.2
	Cdc2^{B47}	22	1316	3.3
CKS30A	*Cks30A*^{RA74}	56	777	14.4
	Cks30A^{KO}	57	1333	8.2
Cdc20	*cort*	42	1626	5.2
Cyclin B	*CycB*^{2}	66	569	23.2
Cyclin B3	*CycB3*^{L6540}	18	1120	3.2
	CycB3^{2}	23	1367	3.4
CDC20	*fzy*^{1}	61	2044	6.0
	fzy^{6}	84	915	18.4
	fzy^{7}	61	1045	11.7
WEE1	*myt*^{R3}	18	741	4.9
Cdc25	*twe*^{1}	55	1130	9.7
	twe^{1}	32	960	6.7
WEE1	*wee*^{DS1}	14	988	2.8
	wee^{ES1}	10	874	2.3
Kinetochore				
CENP-C	*Cenp-C*^{IR35}	78	3319	4.7
NSL1	*Kmn1*^{G0237}	14	1361	2.1
NUF2	*Nuf2*^{EY18592}	23	2667	1.7
SPC25	*Spc25*$^{A34\text{-}1}$	60	1350	8.9
KNL1	*Spc105R*^{1}	20	2030	2.0
Motor protein/spindle				
MAST	*chb*^{4}	30	1169	5.1
CENP-E	*cmet*^{04431}	14	1257	2.2
Dynein	*dhc*$^{4\text{-}19}$	104	2359	8.8
	dhc$^{6\text{-}10}$	64	1702	7.5
PRC1	*feo*^{EA86}	4	633	1.3
NCD	*ncd*^{1}	209	1287	32.5
RAN	*ran*^{G0075}	10	441	4.5
Sentin	*ssp2*^{136}	56	2563	4.4
	ssp2^{32}	31	2692	2.3
Cohesion				
ORD	*ord*^{10}	20	2010	2.0
	ord^{5}	8	846	1.9
	ord^{3397}	132	3507	7.5

Securin	*pim*^{IL}	14	965	2.9
SMC1	*SMC1*^{exc46}	28	893	6.3
Separase	*sse*	9	431	4.2
Three Rows	*thr*^{3}	33	1318	5.0
Checkpoint				
MPS1	*ald*^{c3}	47	1393	6.8
	ald^{B4-6}	32	1976	3.2
BUBR1	*BubR1*^{k03113}	5	980	1.0
ZW10	*zw10*^{1}	13	2671	1.0
CPC/ POLO				
Aurora B	*aurB*$^{2A43.1}$	26	2139	2.4
	aurB$^{49-149}$	74	1904	7.8
	aurB$^{35.33}$	13	2273	1.1
	aurB^{1689}	9	2397	0.8
Aurora A	*aurA*$^{87Ac-3}$	7	951	1.5
Survivin	*Det*^{e01527}	8	436	3.7
INCENP	*Incenp*$^{18.197}$	52	2955	3.5
	Incenp$^{22.68}$	111	1602	13.9
	Incenp^{QA26}	49	2555	3.8
	Incenp^{3747}	86	2978	5.8
POLO	*polo*$^{16-1}$	13	2644	1.0
	polo$^{16-1}$	1	537	0.4
Cytokinesis				
ASP	*asp*^{1}	7	1227	1.1
Four wheel drive	*fwd*^{2}	53	855	12.4
Pavarotti/MLP1	*pav*^{B200}	24	1260	3.8
Subito/MKLP2	*sub*^{1}	144	1179	24.4
	sub^{1} *(18*^{o}*)*	55	1573	7.0
Twinstar/ Cofilin	*tsr*^{1}	25	840	5.8
RacGAP50C	*tum*^{AR2}	10	2111	0.9
	tum^{DH15}	40	2710	2.9

Table S2: Spindle phenotypes and knockdown of shRNA lines used in this study

GENOTYPE	**Knockdown of mRNA (%)** [1]	***tubP-GAL4*** [2]	***matalpha4-GAL-VP16*** [2]	**% abnormal spindles** [3] **(N)**	**P-value** [4]
Wild type	NA	Viable	Fertile	0 (30)	-
polo GL00014	36	lethal	sterile	70 (31)	0.001
polo GL00512	9	lethal	sterile	100 (9)	0.001
Rho1 HMS00375	28	lethal	sterile	40 (43)	0.0001
sticky GL00312	35	lethal	sterile	30 (38)	0.0016
RhoGEF2 HMS01118	11	lethal	sterile	6 (18)	0.375
pbl GL01092	6	lethal	sterile	10 (21)	0.165

[1] Effect on mRNA expression evaluated by qRT-PCR (see Materials and Methods)

[2] Phenotype when crossed to the indicated GAL4 expressing line.

[3] Abnormal spindles were scored as any spindles that have frayed microtubules, not tapered poles or disorganized central spindle.

[4] Fisher's exact test was used to calculate the P-values compared to wild-type

File S1: Mapping of synthetic lethal mutation *27.89*

27.89 is located between the visible recessive markers dumpy and black

Recombination mapping was done by isolating recombinants between the *27.89 sub*^{131} chromosome and a chromosome that contained eight 2nd chromosome recessive visible phenotype markers: *aristaless* (*al*), *dumpy* (*dp*), *black* (*b*), *purple* (*pr*), *cinnabar* (*cn*), *curved* (*c*), *plexus* (*px*), *and speck* (*sp*) (Figure S 3). Flies that have had a crossover between the two chromosomes were identified by crossing to another chromosome with all of the markers. Crossovers were then tested to see if the *27.89* mutation remained on the recombinant chromosome by crossing to the *sub*^{1} allele and checking for synthetic lethality. Using the knowledge of which crossovers retained *27.89* one could deduce whether the mutation is to the left or right of each marker.

For the mapping of *27.89*. 59 recombinants were isolated. Nearly all of the recombinants that crossed over to the left of *dp* (the *al* recombinants) contained *27.89*. Most critically, the recombinants that crossed over in between *dp* and *b* (both the *al dp* recombinants as well as the double crossover *b pr cn* recombinants) showed a mixture of having or lacking *27.89*. These data suggest that 27.89 is likely located in between *dp* and *b.*

Mapping 27.89 to a 303 kilobase region using Single Nucleotide Polymorphisms

To map *27.89* at higher resolution, we used single nucleotide polymorphisms (SNPs) between *dp* and *b* (CHEN *et al.* 2008; CHEN *et al.* 2009). We isolated recombinants between the *27.89* chromosome and a chromosome of a different background so that there would be a large number of SNPs between the chromosomes. The other chromosome was marked with a Minos element (*Mi[GFP]*) inserted just to the left of *subito* (*sub*). Each individual recombinant was

tested for synthetic lethality and the location of the crossover relative to the SNP was determined by PCR followed by a restriction enzyme digest or sequencing of the amplified DNA (Figure S 4). For this SNP mapping scheme, a total of 594 recombinants that were al^+ dp^+ and GFP^- were collected from *al dp 27.89/Mi[GFP]* females. These were selected to isolate recombinants between *dumpy* and the Minos element while ensuring sub^{131} remained on the chromosome.

The SNP marker 939 was used to map the recombinants because is located just to the left of *black* and it was used to discard recombinants that occurred between *black* and *Mi[GFP]*. Similarly, the SNP 865 was used between it was located between *dumpy* and 939. The finding that 65 out of 66 recombinants that crossed over to the right of the SNP 939 were not synthetically lethal (i.e. they did not contain *27.89*), while all 45 of the recombinants that crossed over to the left of SNP 865 were synthetic lethal (i.e. they all contained *27.89*), is consistent with the previous mapping that *27.89* is between *dp* and *b* (Figure S 4A). More importantly, of the 28 recombinants between 865 and 939, 11 were synthetic lethal when crossed sub^1 and 17 were not. This mixture of recombinant types indicates that *27.89* is located between SNPs 865 and 939.

The 28 recombinants between 865 and 939 were tested with additional SNPs in the region 872, 889, and 894. 15 of the 28 recombinants crossed over between 894 and 939, all of which did not have *27.89*, implying that *27.89* is located to the left or very close to the right of 894 (Figure S 4B). 4 of the 28 recombinants crossed over in between 865 and 872, and all of these crossovers contained the *27.89* mutation suggesting that *27.89* is most likely located to the right or close to the left of 872 (Figure S 4E). The 9 remaining recombinants crossed over between 872 and 894, 7 of which retained *27.89* and 2 of which did not. The SNP 889 further divided these 9, into 6 crossovers between 872 and 889, all of which had *27.89*, and 3 crossovers between 889 and 894, of which one contained *27.89* and 2 did not (Figure S 4C and D). These

data indicate that *27.89* is located between 889 and 894, and likely closer to 889. This is a region of approximately 300 kb.

27.89 exhibits homozygous lethality, yet complements all deficiencies within the region between SNPs 872 and 894

The original *27.89* chromosome contained two mutations, *27.89* and sub^{131}. The sub^{131} allele was removed by isolating recombinants of the *27.89* sub^{131} chromosome as discussed above. By picking cn^{+} c^{-} recombinants (*curved* (*c*) is located a short distance to the left of *sub*) a stock was generated that carried only *27.89*. The recombinant *27.89* cn^{+} c^{-} chromosome was homozygous lethal. This could mean that *27.89* is a homozygous lethal mutation. Another possibility, however, was that there was another EMS induced lethal mutation elsewhere on the chromosome. To check if *27.89* is homozygous lethal or there is another EMS induced lethal on the chromosome, recombinants *al dp 27.89* sub^{131}, *27.89 b pr cn* sub^{131} and *27.89 c* were crossed to each, resulting in much of the original mutagenized chromosome remaining heterozygous. Even after removing much of the mutagenized chromosome we still failed to observe *27.89* homozygotes. Thus, these results support the conclusion *27.89* is homozygous lethal,.

We also attempted to map *27.89* using chromosomal deletions. Using the SNP mapping data, we crossed *27.89* to all deficiencies spanning the distance between SNPs 872 and 894 (Figure S 5). None of these deficiencies failed to complement *27.89* for lethality. To determine if the problem lies with the deficiencies, we acquired known homozygous lethal mutations in genes that the deficiencies are supposed to delete. Complementation tests were done between these mutations and their corresponding deficiencies, and it was determined that all of the deficiencies in the region that had complemented *27.89* failed to complement other known lethal mutations. Therefore, it is possible that *27.89* both fails to generate homozygotes yet is viable

when heterozygous to a deficiency. There are currently two explanations for this result, either *27.89* is a recessive hypermorph, that is viable over a deficiency, or the region between *dp* and *b* where *27.89* itself is located, contains a second site lethal mutation.

References

Chen, D., A. Ahlford, F. Schnorrer, I. Kalchhauser, M. Fellner *et al.*, 2008 High-resolution, high-throughput SNP mapping in Drosophila melanogaster. Nat Methods 5**:** 323-329.

Chen, D., J. Berger, M. Fellner and T. Suzuki, 2009 FLYSNPdb: a high-density SNP database of Drosophila melanogaster. Nucleic Acids Res 37**:** D567-570.

Chou, T. B., and N. Perrimon, 1996 The autosomal FLP-DFS technique for generating germline mosaics in Drosophila melanogaster. Genetics 144**:** 1673-1679.

Gelbart, W. M., M. Crosby, B. Matthews, W. P. Rindone, J. Chillemi *et al.*, 1997 FlyBase: a Drosophila database. The FlyBase consortium. Nucleic Acids Res 25**:** 63-66.

Llamazares, S., A. Moreira, A. Tavares, C. Girdham, B. A. Spruce *et al.*, 1991 polo encodes a protein kinase homolog required for mitosis in Drosophila. Genes & Development 5**:** 2153-2165.